University of Szeged

Faculty of Pharmacy

Department of Pharmacodynamics and Biopharmacy

Ph.D. Thesis

Characterization of antiproliferative and antimetastatic properties of novel androstane derivatives

Ágnes Erika Kulmány Pharm.D.

Supervisor:

István Zupkó Ph.D., D.Sc.

2021

SCIENTIFIC PUBLICATIONS RELATED TO THE SUBJECT OF THE THESIS

I. **Kulmány Á E**, Frank É, Kovács D, Kirisits K, Krupitza G, Neuperger P, Alföldi R, Puskás L G, Szebeni G J, Zupkó I: Antiproliferative and antimetastatic characterization of an exo-heterocyclic androstane analog against human breast cancer cell lines. *Biomedicine & Pharmacotherapy*, 2021; 140: 111728
IF: 6.529 / Q1 doi: 10.1016/j.biopha.2021.111728

II. **Kulmány Á E**, Frank É, Papp D, Szekeres A, Szebeni G J, Zupkó I: Biological evaluation of antiproliferative and anti-invasive properties of an androstadiene derivative on human cervical cancer cell lines. *The Journal of Steroid Biochemistry and Molecular Biology*, 2021; 214:105990
IF: 4.292 / Q1 doi: 10.1016/j.jsbmb.2021.105990

III. **Kulmány Á E**, Herman B E, István Zupkó, Sinreih M, Lanišnik Rižner T, Savić M, Oklješa A, Nikolić A; Nagy V, Ocsovszki I, Szécsi M, Jovanović-Šanta S: Heterocyclic androstane and estrane D-ring modified steroids: microwave-assisted synthesis, steroid-converting enzyme inhibition, apoptosis induction, and effects on genes encoding estrogen inactivating enzymes.
The Journal of Steroid Biochemistry and Molecular Biology, 2021; 214:105997
IF: 4.292 / Q1 doi: 10.1016/j.jsbmb.2021.105997

ADDITIONAL PUBLICATIONS NOT RELATED TO THE SUBJECT OF THE THESIS:

1. Bús Cs, **Kulmány Á***, Kúsz N, Gonda T, Zupkó I, Mándi A, Kurtán T, Tóth B, Hohmann J, Hunyadi A, Vasas A: Oxidized juncuenin B analogues with increased antiproliferative activity on human adherent cell lines: semisynthesis and biological evaluation. *J. Nat. Prod.* 83, 11:3250–3261 (2020)
   IF: 4.050 / D1 doi: 10.1021/acs.jnatprod.0c00499

2. Kuskucu M, Akyildiz V, **Kulmány Á**, Ergün Y, Zencir S, Zupko I, Durdagi S, Zaka, M, Sahin K, Orhan H, Topcu Z: Structural modification of ellipticine derivatives with alkyl groups of varying length is influential on their effects on human DNA topoisomerase II: a combined experimental and computational study. *Med. Chem. Res.* 29, 2:189-198 (2020)
   IF: 1.965 / Q2 doi: 10.1007/s00044-019-02472-9

3. Mótyán G, Gopisetty M, Kiss-Faludy R, **Kulmány Á**, Zupkó I, Frank É, Kiricsi M: Anti-cancer activity of novel dihydrotestosterone-derived ring A-condensed pyrazoles on androgen non-responsive prostate cancer cell lines. *Int. J. Mol. Sci.* 20: 2170 (2019)
   IF: 4.556 / Q1 doi: 10.3390/ijms20092170

4. Hammadi R, Kúsz N, Waweru P, **Kulmány Á**, Zupkó I, Orvos P, Tálosi L, Hohmann, J, Vasas A: Isolation and pharmacological investigation of compounds from Euphorbia matabelensis. *Nat. Prod. Commun.* 14, 7:1-5 (2019)
   IF: 0.468 / Q3 doi: 10.1177/1934578X19863509

5. Latif A, Gonda T, Vágvölgyi M, Kúsz N, **Kulmány Á**, Ocsovszki I, Zomborszki Z, Zupkó I, Hunyadi A: Synthesis and in vitro antitumor activity of naringenin oxime and oxime ether derivatives. *Int. J. Mol. Sci.* 20: 2184 (2019)
   IF: 4.556 / Q1 doi: 10.3390/ijms20092184

*: co-first authorship

6. Kiss A, Wölfling J, Mernyák E, Frank É, Gyovai A, **Kulmány Á**, Zupkó I, Schneider Gy: Stereoselective synthesis of new type of estradiol hybrid molecules and their antiproliferative activities. *Steroids,* 148:63-72, (2019)
   IF: 1.948 / Q2 doi: 10.1016/j.steroids.2019.02.016

7. Fröhlich T, Kiss A, Wölfling J, Mernyák E, **Kulmány ÁE**, Minorics R, Zupkó I, Leidenberger M, Friedrich O, Kappes B, Hahn F, Marschall M, Schneider Gy, Tsogoeva SB: Synthesis of artemisinin−estrogen hybrids highly active against HCMV, P. falciparum, and cervical and breast cancer. *ACS Med. Chem. Lett.* 9, 11:1128-1133 (2018)
   IF: 3.737 / Q1 doi: 10.1021/acsmedchemlett.8b00381

8. Vágvölgyi M, Martins A, **Kulmány Á**, Zupkó I, Gáti T, Simon A, Tóth G, Hunyadi A: Nitrogen-containing ecdysteroid derivatives vs. multi-drug resistance in cancer: Preparation and antitumor activity of oximes, oxime ethers and a lactam. *Eur. J. Med. Chem.* 144: 730-9 (2017)
   IF: 4.833 / Q1 doi: 10.1016/j.ejmech.2017.12.032

Cumulative impact factor: 41.226

*: co-first authorship

TABLE OF CONTENTS

1 INTRODUCTION

1.1 Epidemiology of malignant disorders

Cancer represents one of the major health burdens and a leading cause of mortality worldwide, responsible for millions of deaths annually. Cancer therapy and research towards new anticancer agents has become the focus of drug development since the 1950s, when chemotherapy was introduced and the discovery and subsequent clinical use of novel antibiotics made most cases of bacterial infections manageable.[1,2]

The latest survey of the Global Cancer Observatory (GLOBOCAN) series – published by International Agency for Research on Cancer (IARC) – estimated 19.3 million new cancer cases and 9.6 million cancer-related deaths in 2020 (**Figure 1** and **2**). According to these data, one in five men or women suffer from cancer during their lifetime and one in eight men or one in eleven women succumb to cancer-related illness. The analysis of epidemiological data for the last twenty years indicates increasing trends in cancer emergence: approximately 10.1 million new cancer cases and 6.2 million deaths were reported in 2000, which – compared to the latest predictions – corresponds to a ~91% and a ~61% increase in absolute numbers, respectively.[1,3–7]

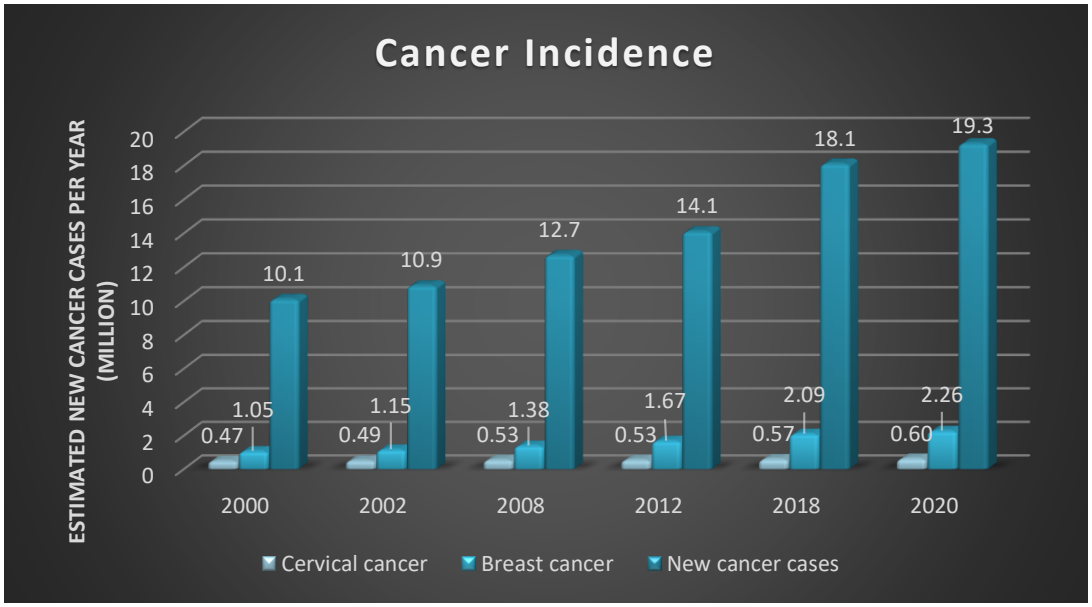

Figure 1. Global cancer incidence from 2000 to 2020, based on GLOBOCAN cancer statistics of World Health Organization (WHO).[1,3–7]

Based on these estimates, the global cancer burden may even reach 28.4 million cases by 2040, a 47% rise from 2020. Besides the increasing numbers, this comprehensive overview – summarising the available incidence and mortality data of 36 cancer types collected from the local registries of 185 countries – revealed causative factors, regional differences and emphasized the leading role of breast and gynaecological cancers among women in incidence and mortality profiles globally.[1]

The complex pathophysiology of breast and gynaecological malignancies has not been completeley understood, and is still in forefront of medical research; nevertheless, several risk factors have been identified so far. These hereditary (e.g. mutation of BRCA1/BRCA2 genes), hormonal (higher overall estrogen exposure, nulliparity, late age at first childbirth, long-term hormone therapy), and environmental (Western-style diet, obesity, alcohol consumption, external radiation, human papilloma virus [HPV] infection) factors provoke the mutation in the DNA content of cells, leading to the evolution of novel functions to avoid programmed cell death and the suppressor mechanisms of cell proliferation.[8–11]

Among females, breast cancer is the most frequently diagnosed type and the principal cause of cancer-related deaths, responsible for 2.26 million new cases and 685,000 deaths, while cervical neoplasms are the fourth most common, both in incidence and mortality, with approximately 604,000 new cases and 342,000 deaths.[3] These two types of malignancies dominate the cancer-related mortality of women in majority of the investigated countries, i.e. breast cancer in 110 countries and cervical cancer in 36 countries.[1]

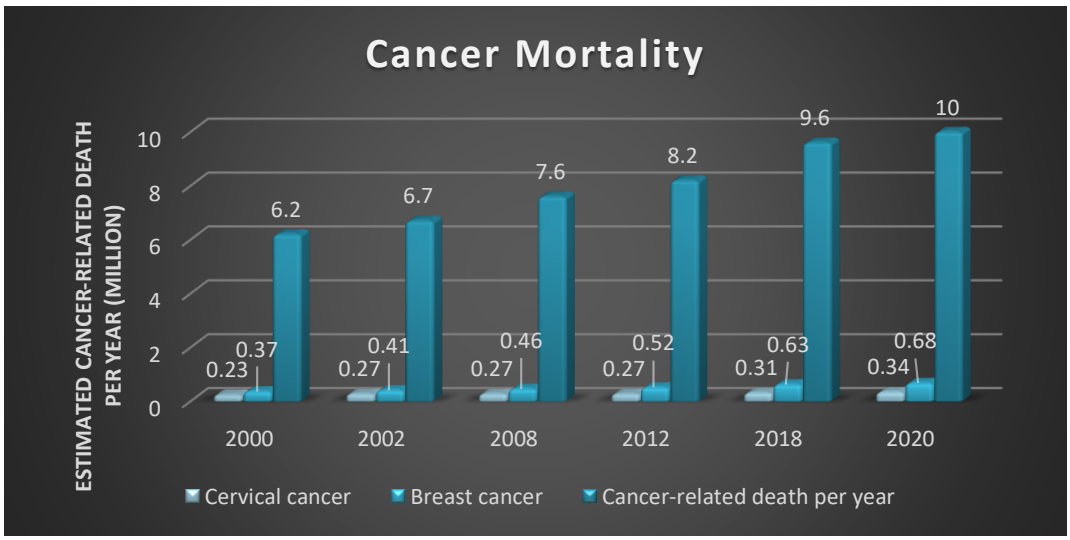

Figure 2. Mortality of cancer from 2000 to 2020 based on GLOBOCAN database of WHO.[1,3–7]

Regarding the causative factors, more than 97% of cervical tumors are caused by 12 oncogenic types of the HPV virus, especially the HPV16 and HPV18 strains, which are the cardinal co-factors of cervical intraepithelial neoplasia (CIN) and cancer in more than 70% of cases. Despite population-based screening programs in developed countries and clinically proven, highly effective HPV vaccines (bivalent, quadrivalent and nonavalent types), which have been commercially available since 2006, cervical cancer is still a global health issue.[12–17]

Although a very high proportion of cancer cases may be treated successfully with improved survival outcome by early diagnosis (owning to milder symptoms or asymptomatic characteristic of the early stages), due to the lack of resources and protocols in many countries, neoplasms are often identified only in their advanced stages.[18,19] Moreover, success of the therapy is limited by *de novo* or acquired resistances against anticancer drugs. For example, 70% of breast cancers express hormone receptors, but 30% of these women are threatened by poor response to endocryn therapy or the risk of recurrence. In numbers, according to the GLOBOCAN survey, 2.26 million women have diagnosed with breast cancer in 2020, so approximately 475 000 patients have a chance to failed first line therapy in subsequent years.[20,21] Furthermore, overall response rate of patients with recurrent or metastatic cervical cancer to combination therapy of cisplatin and paclitaxel – which is a standard chemotherapeutic regimen in these cases – is only 29.1%–67.0%.[22]

Besides rapid advancement in preventive, diagnostic and therapeutic strategies, in the light of previously described facts, novel treatment options of breast and cervical tumors are eagerly awaited.

1.2 Steroids: from natural substances to cancer therapy

Biologically active molecules with a steroidal framework constitute a diverse and extensive group of organic compounds. Hundreds of natural derivatives are found in plants, fungi and animals, while preparation of semisynthetic or synthetic analogues is one of the prominent fields of pharmaceutical research.

Without attempting to be comprehensive, steroidal compounds may be classified into five distinct groups, depending on number of carbon atoms make up their backbone:

The cholestane framework – containing 27 carbons (C27) and various opportunities of substituation – is a core of several important organic substances, such as cholesterol, which has essential role in fluidity of biological membranes and serves as a precursor of hormone sythesis in animals and humans.[23] Ergosterol is found in the cell membrane of fungi and protozoa, with the same functions like cholesterol in animal cells, and this difference serves as basis of several antifungal therapies.[24] Furthermore, these type of molecules establish an outstandingly diverse group of secondary plant metabolites with a broad spectrum of biological activities (e.g., antihypertensive, antiasthmatic, anticancer activities among others). Accordingly, dietary intake of some of these compounds, such as β-sitosterol (the most abundant), campesterol and stigmasterol, may explicate favorable effects on several negative health conditions, for instance mitigating the risk of hormone dependent breast cancer.[25–27]

The structure of cholane steroids comprises of 24 carbons (C24), their main physiological function being the constituents of bile acids and facilitation of fat metabolism (e.g. cholic acid, lithocholic acid). Moreover, synthetic anticancer ephrin type-A receptor 2 (EphA2) antagonist derivatives and analogues with brassinosteroid-like plant hormone properties with cholane skeleton have also been described.[28,29]

Sexual steroids (estrogens, progestogens, and androgens) are essential parts of human hormonal system. These molecules are responsible for proper growth in both sexes, the development of secondary sex characteristics, the maintenance of normal reproductive system, and they also play a crucial role in the function of many organ system, including cardiovascular system, central nervous system and the musco-skeletal system among others.[30–33] Plenty of these compounds, as well as their semi-synthetic and synthetic derivatives, are used for therapeutic purposes, including anabolics, hormonal contraceptives or as part of hormone replacement therapy (HRT). Owing to their lipophilic estrane (C18), androstane (C19) and

pregnane (C21) skeletons, these molecules have favorable pharmacokinetic and pharmacodynamic properties, they can easily penetrate through biological membranes, bind to specific nuclear receptors and exert their pharmacological effects on gene expression.[34]

Besides their physiological impacts, sexual steroids are also involved in the development of numerous hormone-dependent malignancies, such as prostate, breast, endometrial cancer or hormone-independent types, e.g., bladder, lung, colorectal and brain tumors as well.[35–37] In these cases, reduction of hormonal activity is essential in order to decelerate or inhibit the progression of cancer. As enzymes of steroid biosynthesis as well as their nuclear receptors require ligands with appropriate structural units, a very large number of drugs and drug candidates have modified steroidal backbones.[38,39] Among the therapeutically-applied enzyme inhibitors, exemestane, an aromatase inhibitor used in estrogen-dependent breast cancer, fulvestrant, an antiestrogenic compound, and abiraterone, an inhibitor of CYP17A1 applied in prostate carcinoma, are noteworthy.[40–43]

Recent studies suggest that some natural androstanes, as well as their A- or D-ring modified derivatives are able to inhibit proliferation of breast or gynaecological cancer cells, induce cell cycle disruptions and have proapoptotic, antimigratory and antimetastatic properties, without hormonal or antihormonal characteristic (**Figure 3**). Dehydroepiandrosterone, a natural intermediate of steroid biosynthesis, considerably inhibits the proliferation of both HPV-positive and HPV-negative human cervical cancer cells and reduce their adhesive and migratory capacities via an estrogen and androgen independent pathway.[44,45] From semi-synthetic and synthetic analogues, potent growth inhibitory effect of novel 17-picolyl and 17-picolinylidene androstane derivatives were reported by Jakimov, Adjukovic and Djurendic *et al.* on HeLa, MCF-7, MDA-MB-231, PC3, HT-29 and A549 cell lines, while Scherbakov and co-workers demonstrated similar features of several pyrimidine- and dihydrotriazine-derivatives in the androstane and estrane series on MCF-7 and MDA-MB-231 cell lines.[46–49] Besides their antiproliferative character, some derivatives such as oleandrigenin 3-*O*-acetate analogues, containing a substituated androstane core, and 17α-halogenated 19-nortestosterone compounds induce accumulation of cells in the G2/M and sub-G1 phases of the cell cycle at the expense of the G1 phase on HeLa cells, accompanied by down-regulation of anti-apoptotic (Bcl-2, Mcl-1) and tumorigenic (p53, Src kinase) proteins or significantly elevated caspase activity.[50,51] Due to the fact that metastatic tumors show high

mortality rates, pharmacological prevention of metastasis formation is a novel option of anticancer therapies. Wang *et al.* have demonstrated the pronounced antimigratory and anti-invasive properties of E-salignone amide derivatives – synthesized from epiandrosterone and androsterone – on triple-negative MDA-MB-231 breast cancer cells.[52]

On the basis of these evidences and findings of our previous studies, the most frequent position of modification on androstane skeleton to yield novel antiproliferative agents, are C-2 or C-3 on the A-ring and C-16 or C-17 on D-ring (**Figure 3**).[53,54] Comprehensive analysis of structure-activity relationships proved that the incorporation of bulky heterocyclic moiety on the D-ring may result in promising anticancer drug candidates without hormonal activity.

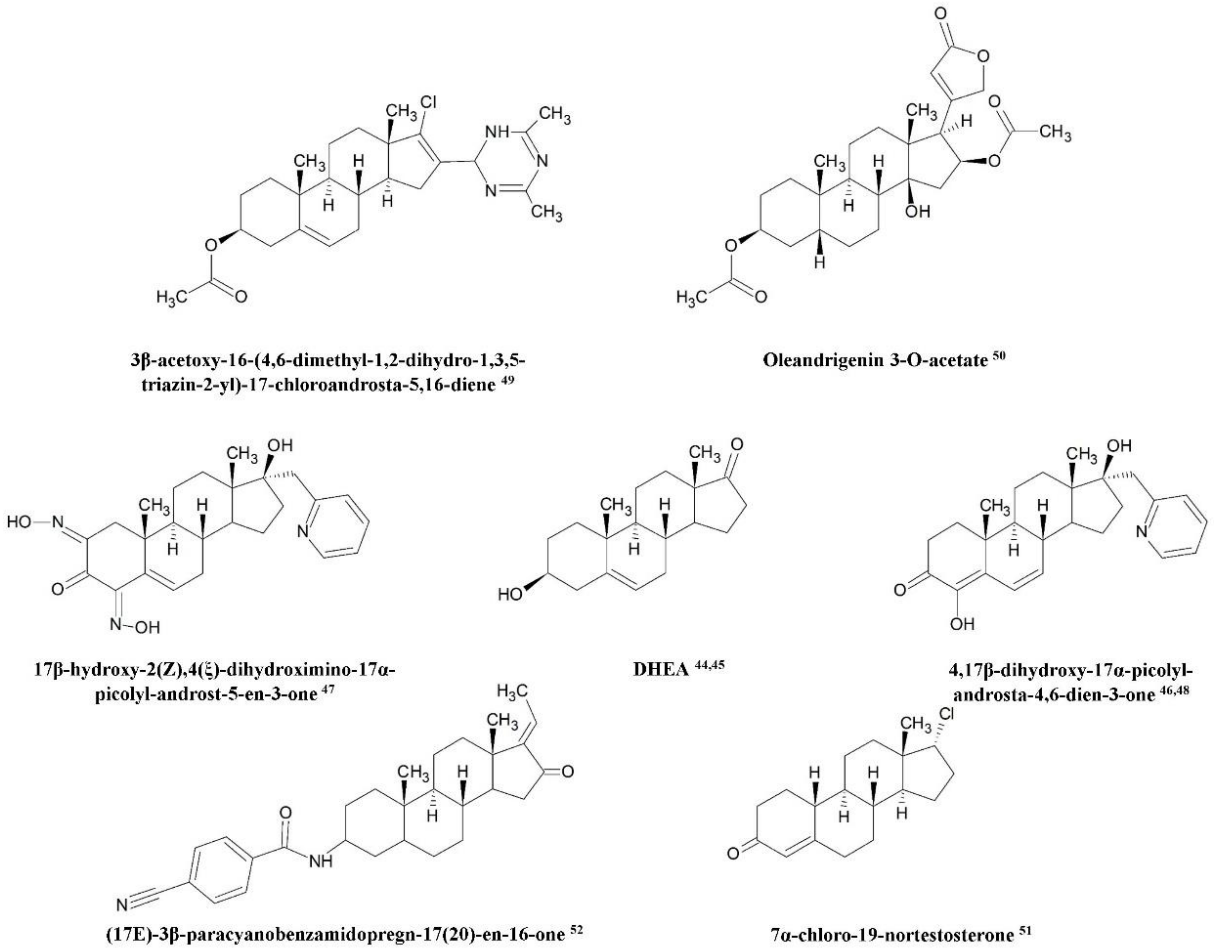

Figure 3. The chemical stucture of leading anticancer androstane derivatives in the described references.

2 AIMS

During our experiments, four novel, heterocyclic, D-ring modified androstane derivatives were examined. 3β-hydroxy-17-[1'-(4''-cyanophenyl)-4'-hydroxymethyl-1'H-pyrazol-3'-yl]androsta-5,16-diene exerted pronounced antiproliferative properties on breast cancer cell lines as reported previously.[55] The aim of the present study was to examine the antiproliferative and antimetastatic characteristics and the underlying mechanism of action of these promising compounds with *in vitro* and *in vivo* experiments on breast and gynaecological tumor cell lines.

The purposes of the performed experiments were as follows:

- Caracterization of antiproliferative properties of the tested compounds on breast and gynaecological cancer cell lines, and the determination of their IC_{50} values by standard MTT assay.
- Estimation of tumor selectivity indices on all of the investigated cell lines compared to a non-cancerous cell line (NIH/3T3).
- Detection of apoptosis-inducing effects of the tested compounds, and their pathway using Hoechst/propidium iodide and Annexin V/propidium iodide fluorescent double staining methods, cell cycle analysis, colorimetric determination of caspase-3 activity and mitochondrial membrane potential assay (JC-1 assay).
- Demonstrating the possible androgenic/antiandrogenic activity of the tested compounds, owing to the androstane skeleton by yeast androgen screening assay (YAS).
- Examination of the inhibitory effects of the tested compounds to the early steps of metastasis formation such as migration, invasion and intravasation, carrying out wound-healing, Boyden chamber and circular chemorepellent-induced defects (CCIDs) assays.
- Analysis of expression level of tumor markers upon treatment with the tested compounds.
- Investigation of *in vivo* administration of the tested compounds on the 4T1 ortothopic mouse breast cancer model.

3 MATERIALS AND METHODS

3.1 Chemicals

Synthesis and chemical characterization of 3β-hydroxy-17-[1'-(4''-cyanophenyl)-4'-hydroxymethyl-1'H-pyrazol-3'-yl]androsta-5,16-diene (compound **1**) were carried out by Éva Frank *et al.* as reported previously.[55] Tetrazole (compound **2** and **3)** and triazole (compound **4)** derivatives were prepared by the colleagues of the Department of Chemistry, Biochemistry and Environmental Protection, University of Novi Sad, Serbia. The chemical structure of these molecules are presented in **Figure 4**.

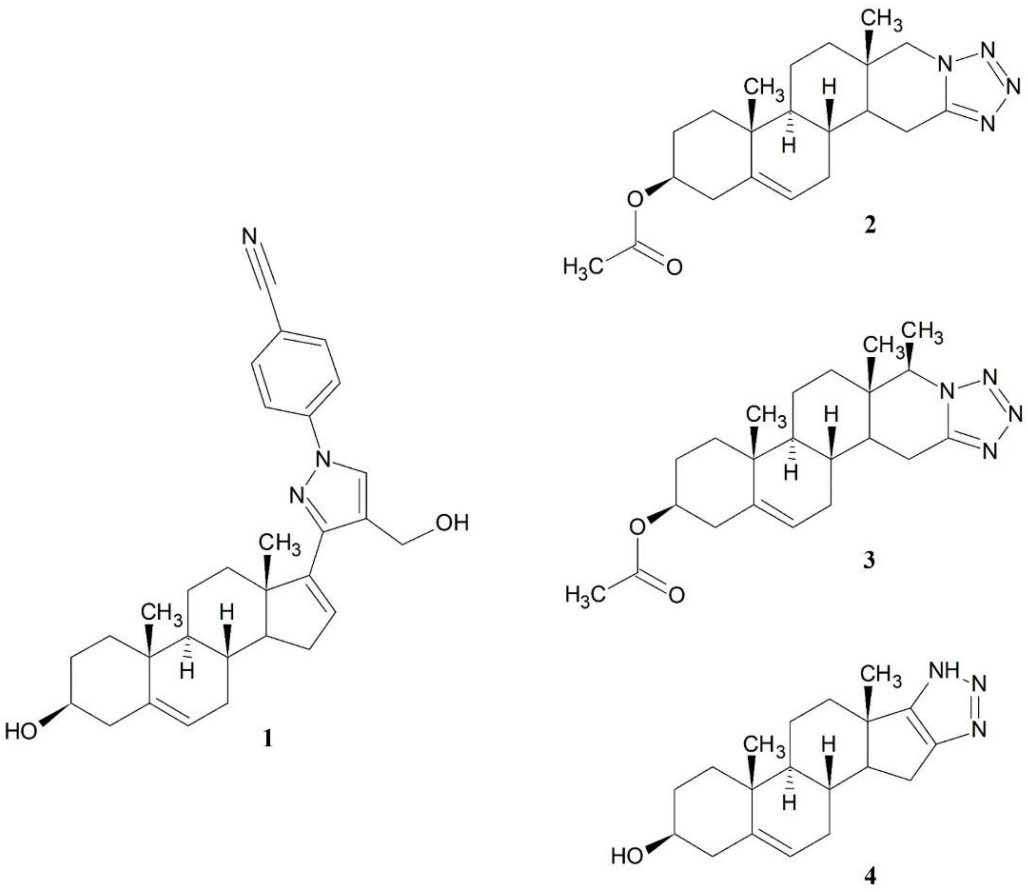

Figure 4. Chemical stuctures of the tested compounds (**1-4**)

3.2 Cell lines

HeLa, A2780, MCF-7, T-47D, MDA-MB-231, MDA-MB-361 and NIH/3T3 cell lines were purchased from ECACC (European Collection of Cell Cultures, Salisbury, UK), 4T1, SiHa and C33A cell lines were acquired from ATCC (American Tissue Culture Collection,

Manassas, VA, USA). The T1S1/iLEC cell line was obtained from the Department of Pathology, Medical University of Vienna (Vienna, Austria). HeLa, SiHa, C33A, A2780, MCF-7, T-47D, MDA-MB-231 and NIH/3T3 cells were maintained in Eagle's Minimal Essential Medium (EMEM), supplemented with 10% fetal bovin serum (FBS), 1% non-essential amino acid (NEAA) mixture and 1% penicillin, streptomycin and amphotericin B mixture at 37°C in a humidified carbon dioxide (CO_2) atmosphere. iLEC cells were grown in EGM-2MV (EGM-2MV BulletKit, Lonza, Basel, Switzerland) medium under the same conditions. MDA-MB-361 cells were cultivated in L-15 medium, complemented with 20% FBS, 1% NEAA mixture and 1% antibiotic/antimicotic mixture at 37°C, under humidified carbon dioxide-free circumstances. 4T1 mouse breast cancer cells were cultured in RPMI medium containing 10% FBS, 1% NEAA mixture and 1% antibiotic solution in CO_2 incubator at 37°C. All media, supplements, chemicals and kits used during experiments and cell cultures, if otherwise not specified, were purchased from Sigma-Aldrich Ltd. (Budapest, Hungary).

Cell line	Origin and main characteristic
MCF-7	human breast adenocarcinoma, derived from a pleural effusion, which expresses estrogen and progesteron receptors
T-47D	human ductal carcinoma of the breast, derived from a pleural effusion, which expresses estrogen and progesterone receptors with different progesterone response than MCF-7
MDA-MB-361	estrogen and HER2 receptor positive human breast cancer cell line, derived from a brain metastasis
MDA-MB-231	triple negative human breast cancer cell line
HeLa	HPV-18 positive human cervical carcinoma cell line
SiHa	HPV-16 positive human cervical carcinoma cell line
C33A	HPV-negative human cervical carcinoma cell line
A2780	human ovarian carcinoma cell line, derived from an untreated patient
T1S1/iLEC	immortalized human lymphatic endothelial cell line
NIH/3T3	mouse embryonic fibroblast cell line
4T1	highly tumorigenic and invasive breast cancer cell line from BALB/cfC3H mouse

Table 1. Origin and main characteristic of the utilized cell lines.

3.3 MTT-assay (antiproliferative assay)

Proliferation and viability of cells upon treatment with the test compounds were investigated by the standard MTT assay.[56] All cell types were maintained under the cell culturing circumstances described previously, and were seeded into 96-well plates at a density of 5,000 cells/well, except for the MDA-MB-361 and C33A cells, as they were plated at a density of 10,000 cells/well, and were treated with increasing concentrations of the test substances (0.1-30 μM). Untreated cells were used as a control and final concentration of dimethyl sulfoxide (DMSO) from the stock solutions was lower than 0.3%, so it exerted no substantial effect on cell proliferation. After 72 h of incubation, 3-(4,5-dimethylthiazol-2-yl)-2,5-diphenyltetrazolium bromide (MTT) solution (5 mg/mL in phosphate buffer) was added to the wells for 4 h and the precipitated, blue formazan crystals were dissolved in 100 μL DMSO. Finally, absorbances, reflected the number of viable cells, were recorded by a microplate reader (Stat Fax 2100, Awareness Technologies, Westport, CT, USA) at 545 nm and normalized six-point dose-response curves were evaluated by GraphPad Prism 5.01 software (GraphPad Software, San Diego, CA, USA).

3.4 Hoechst/Propidium iodide fluorescent double staining

Apoptosis or necrosis-related changes in cell morphology and membrane integrity were investigated by Hoechst 33258 and propidium iodide (PI) fluorescent staining.

Suspension of MCF-7 and SiHa cells were seeded into 96-well plates (5,000 cells/well) and were treated with increasing concentrations (1, 2 and 4 μM) of compound **1** for 24 h. After treatment period, cells were stained by lipophilic Hoechst 33258 (5 μg/ml) and hydrophilic PI (3 μg/ml) solution for 1 hour in the dark, under cell culturing conditions described above. Next, the medium was refreshed on samples, and images (at least 10 per condition) were taken by the QCapture Pro software (QImaging, Surrey, BC, Canada) and a Nikon Eclipse TS100 fluorescence microscope (Nikon Instruments Europe B.V., Amstelveen, The Netherlands) equipped with appropriate filters for Hoechst 33258 (excitation: 360/40 nm bandpass filter, emission: 460/50 nm bandpass filter and 400 nm dichromatic mirror) and for PI (excitation: 500/20 nm bandpass filter, emission: 520 nm longpass filter and 515 nm dichromatic mirror). Nuclei emitting fluorescence were counted and the proportion of intact, apoptotic and necrotic cell populations were expressed as percentages.

3.5 Apoptosis Assay

For more detailed separation of early- and late apoptotic subpopulations, Annexin V-Alexa488/PI fluorescent staining, complemented with flow cytometric detection – which is appropriate to analysis of larger event numbers per sample – were used.

MCF-7, MDA-MB-231 and SiHa cells were seeded at a density of 80,000 cells/well, while C33A cells were plated at a density of 120,000 cells /well into 24 well cell culture plates and were treated with different concentrations (1, 2, 4 and 8 μM) of the test compound (**1)** for 24 h. Next, cells were washed with PBS, harvested with trypsin and pooled with the collected supernatants. Samples were centrifuged at 300 × *g* at room temperature for 5 minutes, and pellets were resuspended in Annexin V binding buffer (0.01 M HEPES, 0.14 M NaCl and 2.5 mM $CaCl_2$) accompained by staining procedure with Annexin V-Alexa488 (LifeTechnologies, Waltham, MA, USA) and propidium iodide (10 μg/ml) solution in the dark at room temperature for 15 minutes. For each sample, 10 000 events were detected by FACSCalibur cytofluorimeter (BD Biosciences, San Jose, CA, USA) and data were analysed by CellQuest™ software (Becton Dickinson, Franklin Lakes, NJ, USA).

3.6 Cell cycle analysis

In order to determine the influence of compound **1** to cell cycle of breast- and cervical tumor cells, cell cycle analyses were performed on four cell lines as described previously.[57] Briefly, MCF-7, MDA-MB-231, SiHa and C33A cells were seeded onto 24-well plates (80,000 cells/well or 120,000 cells/well) and were exposed to the same concentration range (1, 2, 4 and 8 μM) of our drug candidate described for the previous experiment for 48 h or 72 h. The samples were washed with phosphate-buffered saline (PBS), collected, pooled with the corresponding supernatants and centrifuged at 300 × *g* at room temperature for 5 min. The DNA content of resuspended cells were labelled with PI in DNA staining solution (10 μg/mL PI, 0.1% Triton-X, 10 μg/mL RNase A, and 0.1% sodium citrate dissolved in PBS) for 30 min in the dark, at room temperature. Analysis of at least 20,000 events/sample were carried out by the FACSCalibur flow cytometer and the Kaluza Analysis Software (Beckman Coulter, Brea, CA, USA). Untreated cells were applied as control and hypodiploid sub-G1 phases were considered as natural outcome of apoptosis.

3.7 Determination of caspase-3 activity

Changes in activity of caspase-3 – an executioner enzyme of apoptotic programmed cell death – were determined with a commercially-available colorimetric assay.

SiHa cells were grown in cell culture flasks at a density of 10^7 cells/flask as control and $1{,}5x10^7$ cells/flask as treated samples under standard cell culturing conditions and treated (1, 2 or 4 μM) for 24, 48 and 72 h. Thereafter, cells were collected with a special cell scraper tool and counted. Samples were centrifuged on 940 × *g* at 4°C for 15 min, supernatants were gently removed and cells were lysated by required (100 μL/10^7 cells) amount of lysis buffer of the kit on ice for 20 min. Next, lysates were centrifuged (16.000 × *g*, 4°C, 15 min) and 5 μL portions of the supernatants were incubated overnight with 10 μL substrate (acetyl-Asp-Glu-Val-Asp-*p*-nitroanilide) and 90 μL assay buffer in 96-well plate at 37°C according to the manufacturer's protocol. Finally, absorbance values of the colorful substrate cleaved by caspase-3 in samples were detected at 405 nm with a microplate reader.

3.8 Mitochondrial membrane potential assay (JC-1 staining)

By JC-1 staining with flow cytometric detection, activation of the intrinsic pathway of apoptosis via damage of the mitochondrial membrane was demonstrated experimentally, as described previously.[58] MCF-7, MDA-MB-231, SiHa and C33A cells were grown and harvested under standard cell culturing conditions, and were seeded onto 24 well plates (Corning Life Sciences, Corning, NY, USA). From MCF-7 and MDA-MB-231 cell lines, 10^5 cells/well were seeded, while from the SiHa and C33A cell lines, 80,000 and 120,000 cells/well were applied, and the same concentrations (1, 2, 4 and 8 μM) of the test compound were used as in the apoptosis assay. After 12 h (MCF-7, MDA-MB-231) or 24 h (SiHa, C33A) treatment of compound **1**, samples were washed, collected and centrifuged at 600 × *g* for 5 minutes. After that, pellets were resuspended and stained with JC-1 (Chemodex, St. Gallen, Switzerland) solution (5 μg/ml) for 5 minutes at 37°C. Finally, red and green fluorescence of the cells were investigated on FL2 (585/42 nm) - FL1 (530/30 nm) channels by the FACSCalibur flow cytometer. In each analysis, 10,000 events were recorded and data were evaluated by CellQuest™ software.

3.9 Yeast Androgen Screen assay (YAS)

A yeast-based microplate assay (XenoScreen YES/YAS kit, Xenometrix AG, Allschwil, Switzerland) was performed to reveal potential hormonal or antihormonal activity of compound **1**, owing to its androstadiene skeleton. The colorimetric method is based on genetically modified yeast cells (*Saccharomyces cerevisiae*) bearing the sequence of the human androgenic receptor gene integrated into their DNA, as well as an expression plasmid containing the lacZ reporter gene, encoding for the β-galactosidase enzyme and androgen responsive elements. The yeast cells were grown in growth medium of the kit in humidified air at 31°C on an orbital shaker, until the adequate cell density had been reached. Next, they were plated onto assay plates and were incubated in the presence of the CPRG substrate (chlorophenol red-β-D-galactopyranoside) and the test substance (ranging from 1 μM to 10 mM) and/or 5α-dihydrotestosterone (DHT) used as reference agent (ranging from 1 nM to 1 μM), for 2 days. For the purposes of determining the antagonistic effect of the compound, the medium was supplemented with DHT, and flutamide (concentrations ranging from 10 μM to 10 mM) was used as positive control, while for the demonstration of agonistic potency, DHT was applied separately as a reference agent. Androgenic activity triggers the expression of β-galactosidase from the reporter gene and this enzyme can convert the yellow CPRG substrate into a red product. Absorbance of samples were detected at 570 nm and 690 nm and the results were calculated with the Excel calculation workbook by Xenometrix, as based on the manufacturer's protocol.

3.10 Wound-healing assay

As they constitute some of the initial steps of metastasis development, migration of malignant cells was investigated by a wound-healing assay. In our experiments, 20,000 MCF-7 cells per well and 25,000 SiHa cells per well were implanted in special silicon inserts (Ibidi GmbH, Gräfelfing, Germany), which were placed onto 24-well plates in standard EMEM medium, containing 10% FBS. After overnight incubation, inserts were removed cautiously and the confluent monolayers with certain cell-free areas were washed with PBS. Cells were treated with sub-antiproliferative concentrations of compound **1** (MCF-7: 0.1 and 0.3 μM; SiHa: 0.01 and 0.03 μM) in EMEM medium containing 2% FBS, and images were taken by a Nikon Eclipse TS100 microscope 0, 24 and 48 h post-treatment. Untreated cells were used as control

and rate of wound-closure (i.e. reduction in size of the cell-free gaps) were measured by ImageJ software (National Institutes of Health, Bethesda, MD, USA).

3.11 Boyden chamber assay

The anti-invasive potential of compound **1** was tested by the Boyden chamber assay on highly invasive, triple negative MDA-MB-231 breast carcinoma cell line and HPV-positive SiHa cells.

After prehydration of a polyethylene terephthalate (PET) membrane (8 μm pore size) and the thin layer of matrigel basement matrix (2 h, serum-free EMEM) in special Boyden chamber inserts (BioCoat™ Matrigel® Invasion Chambers, Corning Inc, Corning, NY, USA) placed onto a 24 well plate, cell suspension (50,000 cells/insert from both cell lines) prepared in serum-free EMEM with sub-antiproliferative concentrations (MDA-MB-231: 0.1 and 0.3 μM; SiHa: 0.01 or 0.03 μM) of the test substance was nested in the upper compartments. Untreated cells were used as controls, and EMEM medium supplemented with 10% FBS was applied as a chemoattractant in the lower chambers. After 24 h incubation, supernatants and non-invading cells were removed cautiously with a cotton swab. Next, cells were washed with PBS twice, fixed in ice cold 96% ethanol and were stained by 1% crystal violet dye for 30 minutes in the dark. At least 3 images per chamber were taken by the Nikon Eclipse TS100 microscope and the number of invading cells were counted.

3.12 Circular chemorepellent-induced defects assay (CCIDs)

Anti-intravasative properties of compound **1** were studied by a circular chemorepellent-induced defects assay as a 3D, co-culture model for the early steps of metastasis development. Initially, MCF-7 cells suspended in EMEM medium, complemented with standard supplements and a methylcellulose solution in the final concentration of 0.3% in a density of 3000 cells/well was plated onto U-bottom 96-well plates. Plates were centrifuged on 300 × *g* for 15 minutes at room temperature, and incubated for 3 days to form spheroids.

Non-cancerous human lymphendothelial cells (iLEC) were seeded onto 24-well plates and grown to approximately 100% of confluency. Before measurement, iLEC monolayer were stained with CellTracker Green dye (ThermoFisher Scientific, Waltham, MA, USA) for 1 hour at 37°C. The endothelial barriers and selected tumor spheroids were washed with PBS and pre-incubated with compound **1** or defactinib (1, 2, 4, 8 and 16 μM) or epiandrosterone (2, 5, 10,

20 and 40 μM) used as reference agents, for 20 minutes, separately. After pretreatment, the spheroids were placed upon the iLEC cell monolayer and incubated for 4 hours, in the presence of the test compounds. As control samples, spheroids and iLEC monolayer treated by a medium supplemented with 0.1% DMSO were applied. Finally, images of at least 12 spheroids per condition were taken by fluorescent Axiovert microscope (Zeiss GmbH, Jena, Germany) and image analysis of cell-free areas was carried out by Zen Little 2012 software (Zeiss GmbH, Jena, Germany).

3.13 Single cell mass cytometry

Single cell mass cytometry was performed as described previously.[57] Briefly, MDA-MB-231 cells were seeded (4×10^5 cells/well in 6-well plates) and were incubated with 8 μM of compound **1** for 72 h and untreated cells were used as controls. After treatment, cells were washed with PBS, collected by Accutase (Corning Life Sciences, Corning, NY USA) and three technical replicate wells were pooled and were centrifuged (5 min, 350 × *g*) as a sample. Pellets were suspended in PBS and cells were counted by a Bürker chamber and trypan blue viability dye. To demonstrate viability of the cells, cisplatin staining (5 μM 195Pt, Fluidigm, San Francisco, CA, USA) was carried out for 3 min on ice in 300 μL PBS. Samples were diluted with 1,500 μL Maxpar Cell Staining Buffer (MCSB, Fluidigm), centrifuged at 350 × *g* for 5 min and were incubated with TruStain FcX (Biolegend, San Diego, CA, USA), 2.5 μL in 50 μL MCSB (PBS containing blocking proteins) for 10 min to prevent non-specific binding of the antibodies. Samples were centrifuged (350 × *g*, 5 min), suspended in 50 μL MCSB, and the resultant antibody mix (**Table 1**) was added to 50 μL of fresh master pool of antibodies. Some of the applied antibodies were produced by the conjugation of the antibodies with metal tags in-house (anti-CA9, anti-GLUT1, anti-MCT4 and anti-TMEM45A), using a Maxpar metal labelling kit, according to the protocol of the manufacturer (Fluidigm). Prior to the experiment, optimal dilution of the antibodies was ascertained by titration.

Catalogue Number	Supplier	Target	Metal Tag
3170009B	Fluidigm	EGFR	^{170}Er
3156026B	Fluidigm	CD274 (PD-L1)	^{156}Gd
3141006B	Fluidigm	CD326 (EpCam)	^{141}Pr
MAB1418	R&D Systems	GLUT1	^{154}Sm
sc-376140	Santa Cruz Biotech.	MCT4	^{171}Yb
3162027A	Fluidigm	Pan-Keratin	^{162}Dy
3149018B	Fluidigm	CD66-a,c,e	^{149}Sm
3153026B	Fluidigm	Galectin-3 (Gal-3)	^{153}Eu
orb357227	Biorbyt	TMEM45A	^{169}TM

Table 2. Antibodies used for mass cytometry

After 60 min of incubation at 4°C, the cells were washed by 2 mL MCSB and centrifuged at 300 × *g* for 5 min twice, and the pellets were re-suspended in the residual volume. Fixation of the samples was accomplished in 1.6% formaldehyde (freshly diluted from 16% Pierce formaldehyde with PBS, Thermo Fisher Scientific) at room temperature for 10 min. Next, the cells were centrifuged at 800 × *g* for 5 min, and the Cell-ID DNA intercalator (^{191}Ir/^{193}Ir, Fluidigm) in Maxpar Fix and Perm buffer (Fluidigm) was added (1:1,000 dilution) to the samples for overnight incubation at 4°C. After additional washing steps with MCSB, the samples were centrifuged at 800 × *g* for 5 min and the pellets were suspended in 1 mL PBS (for WB injector). For the measurement, the cell number was set to 0.3×10^6/mL in a cell acquisition solution (CAS, Fluidigm), containing 10% EQ Calibration Beads (Fluidigm) and the samples were percolated with 30 µm gravity filter (Celltrics, Sysmex Partec, Kobe, Japan). After manual gating using the ^{191}Ir and ^{193}Ir DNA intercalators, singlets excluded cell debris and aggregates were analysed by the Cytobank platform (Beckman Coulter). Next, cells expressed the examined markers (untreated and subpopulation with enhanced drug-sensitivity [^{195}Pt+]) were manually gated and the t-SNE (t-distributed stochastic neighbour embedding) analysis (iterations = 1,000, perplexity = 30, theta = 0.5), was performed on 1.5×10^4 events. The percentages of cells positive for a specified marker were presented on before-after plots. Three biological replicate experiments were performed and demonstared.

3.14 *In vivo* mouse model of breast cancer

Even the most sophisticated *in vitro* experiments are unable to represent the exact effects of a drug candidate in a living system, such as in body of animals or humans. Therefore, antitumoral properties of our test substance were tested in an orthotopic 4T1 mouse breast

cancer model *in vivo* as reported earlier.[59] The experiments were accomplished in accordance with the EU rules (2010/63/EU) on animal experimentation and ethics. The experimental protocol was approved by the responsible governmental agency (National Food Chain Safety Office) in concordance with the ethical clearance No. XXIX./128/2013.

BALB/c mice (7 animals per group, weighing 18–26 g) were housed in sterile, IVC cage system, equipped with a HEPA filter at ambient temperature of 25°C. At the first day of the experiment, 120,000 4T1 breast carcinoma cells per animal, collected from fresh cell culture and suspended in FBS-free RPMI medium, were injected into the mammary pad of the mice.

On the 12th day of the experiment, animals were randomized into two groups (n=7) and the mean tumor size of each group was between 22 and 25 mm^3. Members of the test group were treated intraperitoneally with 25 mg/kg dose of compound **1** (determined in preliminary toxicology), dissolved in mixture of DMSO : Solutol HS 15 : saline (1:3:10) once per day, five times per week for 2 weeks. Animals of the control group were treated with the vehicle mixture. Tumor size ($d^2 \times D \times 0.5$, where d and D are minor and major tumor diameters, respectively) and body mass were determined daily, and on the 15th day of treatment period, animals were terminated. Finally, weight of the surgically removed tumor tissues were measured.

3.15 Statistical analysis

For statistical analyses, GraphPad Prism version 5.01 software was used. The statistical significance was estimated by one-way analysis of variance (ANOVA), followed by the Dunnett post-test. In the Results section, all data are presented as means ± SEM of at least three replicates. *, ** and *** indicate $p<0.05$, $p<0.01$ and $p< 0.001$ compared to control samples, respectively.

4 RESULTS

4.1 MTT assay

In case of compound **1**, previous experimental data evidenced promising antiproliferative activity on breast cancer cell lines. For further examinations, MTT assay were carried out on three cervical and one ovarian cancer cell lines, and the newly synthesized compound **2, 3** and **4** were tested on four breast cancer cell lines as well. The calculated IC_{50} values (defined as the concentration of the compound which can inhibit cell proliferation by 50% compared to untreated cells) of the test substances and cisplatin used as positive control, are presented in **Table 2**.

Cell line	Calculated IC_{50} value (μM)				
Compound	**1**	**2**	**3**	**4**	**CIS**
HeLa	1.13	>30	>30	>30	13.75
SiHa	0.78	>30	>30	>30	13.51
C33A	1.72	>30	>30	>30	3.09
A2780	2.34	>30	>30	29.58	1.30#
MCF-7	1.40*	>30	>30	>30	5.78#
T47D	1.20*	>30	>30	>30	9.78#
MDA-MB-361	1.60*	>30	>30	>30	3.74#
MDA-MB-231	1.80*	>30	>30	>30	19.13#

Table 2. Calculated IC_{50} values of compound **1-4** and cisplatin (CIS) determined on eight human breast or gynaecological cancer cell lines. * and # are data from literature.[51,55]

Compound **1** exerted considerable antiproliferative activity against breast and cervical cancer cell lines, while compound **2**, **3** and **4** showed no substantial effect on cell proliferation; thus, compound **1** was selected for further experimentation. For comparison, the IC_{50} values of therapeutically applied cisplatin used as reference agent, are presented for the same cell lines.

Furthermore, inhibition of cell proliferation, as well as tumor selectivity, is a crucial concern during the research for novel antineoplastic agents. In order to obtain information about tumor-selectivity, quotients of IC_{50} values obtained on cancerous and non-cancerous (NIH/3T3) cells were prepared (**Table 3.**). In case of compound **1**, these tumor selectivity indices were <1 but >0.1, which indicate moderate selectivity.

Cell line	IC_{50} malignant/IC_{50} NIH 3T3	IC_{50} CIS/IC_{50} NIH 3T3
HeLa	0.301	5.098
SiHa	0.208	5.009
C33A	0.459	1.146
A2780	0.624	0.482
MCF-7	0.373	2.14
T47D	0.320	3.63
MDA-MB-361	0.427	1.39
MDA-MB-231	0.480	7.09

Table 3. Tumor selectivity indices of compound **1** on the utilized cell lines calculated by the following equation: IC_{50} [cancerous]/ IC_{50} [non-cancerous].

4.2 Hoechst/Propidium iodide fluorescent double staining

Changes in cell morphology and the membrane integrity of MCF-7 and SiHa cells were observed 24 h post-treatment. Fluorescent images revealed decreased number of viable cells, and significant elevation in the number of nuclei emitting light blue fluorescence due to DNA condensation in early apoptosis and red fuorescence in secondary necrotic cells with damaged cell membrane in a concentration-dependent manner (**Figure 5**). Statistical evaluation confirmed an increase in early apoptotic cells by 10.9%, and of secondary necrotic nuclei by 16.0% at the highest concentration in MCF-7 cells. In case of SiHa cells, proportion of these subpopulations elevated by 15.2% and 34.2% at the same concentration, respectively.

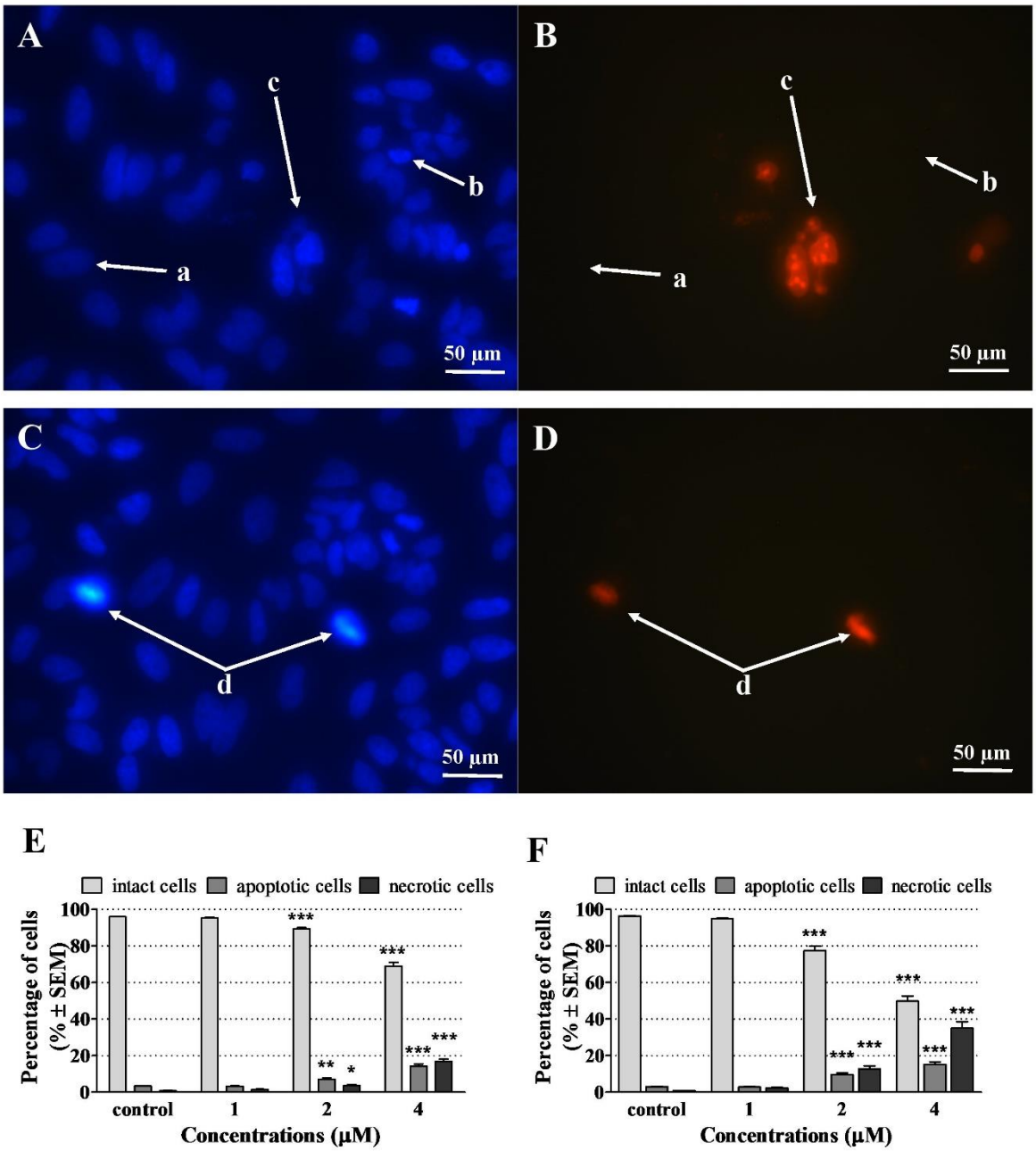

Figure 5. Compound **1** induced apoptosis in breast and cervical cancer cells. Intact (a), early apoptotic (b), late apoptotic (c) and necrotic (d) MCF-7 nuclei exposed to 2 µM of compound **1** for 24 h and stained by Hoechst 33258 (blue fluorescence, A, C) and PI (red fluorescence, B, D) were visualized by fluorescent microscopy at 400× magnification. The ratio of intact, apoptotic and necrotic cell populations is presented in percentage in MCF-7 (E) and SiHa (F) samples. *, ** and *** indicate significant differences between compound **1** treated and untreated control samples at $p<0.05$, $p<0.01$ and $p<0.001$, respectively.

4.3 Apoptosis assay

For detailed assessment of induced apoptotic and necrotic cell populations and to separate early vs. late apoptotic events more precisely, Annexin V-Alexa488/PI fluorescent double staining were performed after 24 h treatment. In all cancer cell lines, compound **1** triggered a concentration-dependent elevation of phosphatidylserine exposure as an indicator of apoptotic process (early apoptosis: AnnV+/PI–; late apoptosis: AnnV+/PI+) without presence of massive necrotic cell population (necrosis: AnnV–/PI+) (**Figure 6**). In case of SiHa cells amount of early and late apoptotic cells increased by 5.4% and 16.8%, while in C33A samples number of early apoptotic cells did not change but late apoptotic events elevated by 35.4% at 8 μM. Furthermore, proportion of the late apoptotic cell populations were significantly elevated in breast cancer cell lines (MCF-7 and MDA-MB-231) by 26.5% and 24.1% at the highest applied concentration, respectively.

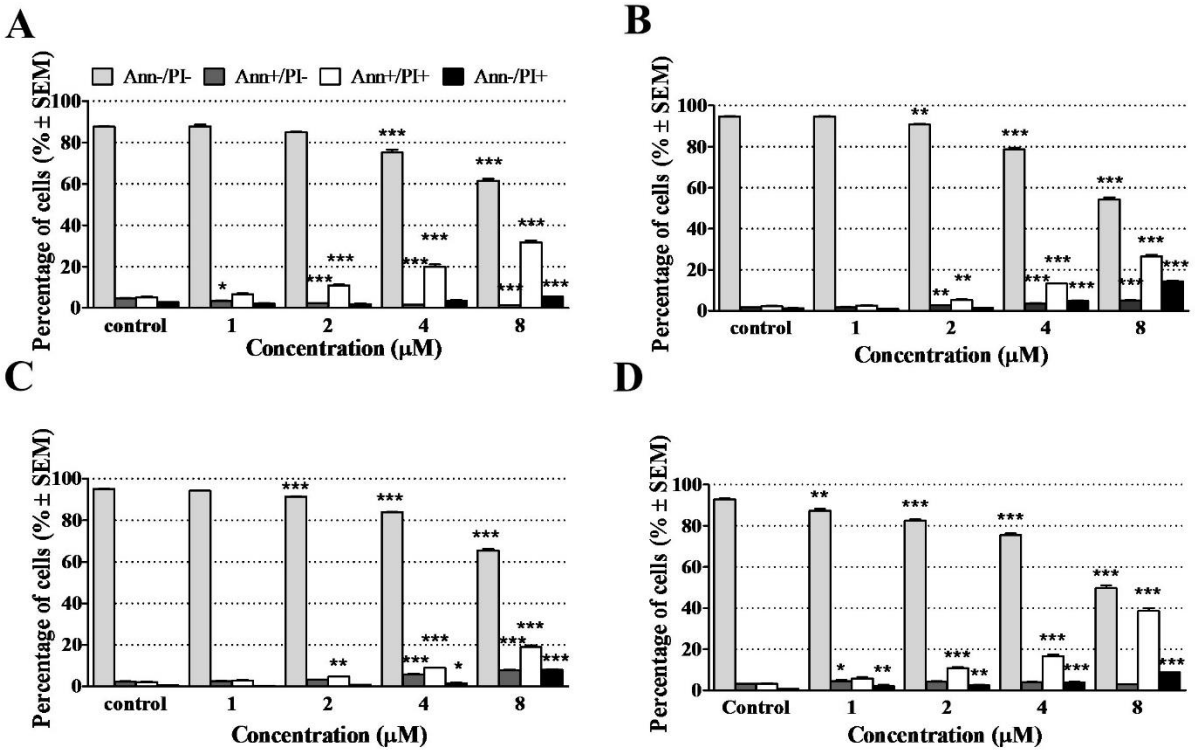

Figure 6. Compound **1** induced accumulation of early and/or late apoptotic cell populations. Changes in intact (AnnV–/PI–), early apoptotic (AnnV+/PI–), late apoptotic (AnnV+/PI+), and necrotic (AnnV–/PI+) populations of MCF-7 (A), MDA-MB-231 (B), SiHa (C) and C33A (D) cells are presented in percentage. Concentration-dependent alterations were observed in the rate of early and late apoptotic and necrotic cell fractions 12 h post-treatment in breast carcinoma and 24 h post-treatment in cervical cancer cell lines. *, ** and *** indicate $p<0.05$, $p<0.01$ and $p<0.001$, respectively.

4.4 Cell cycle analysis

In order to obtain information about mechanism of action, cell cycle disturbances were analysed by flow cytometry. Concentration-dependent elevation of hypodiploid sub-G1 population, regarded as marker of apoptotic process, were recorded at ≥2 μM in all of the four examined cell lines (MCF-7, MDA-MB-231, SiHa, C33A) after 48 h treatment (**Figure 7**). Numerically, compound **1** induced accumulation of natural outcome of apoptosis by approximately 20% in MCF-7, by 14% in MDA-MB-231, by 17% in SiHa and by 17% in C33A cell lines at the highest concentration.

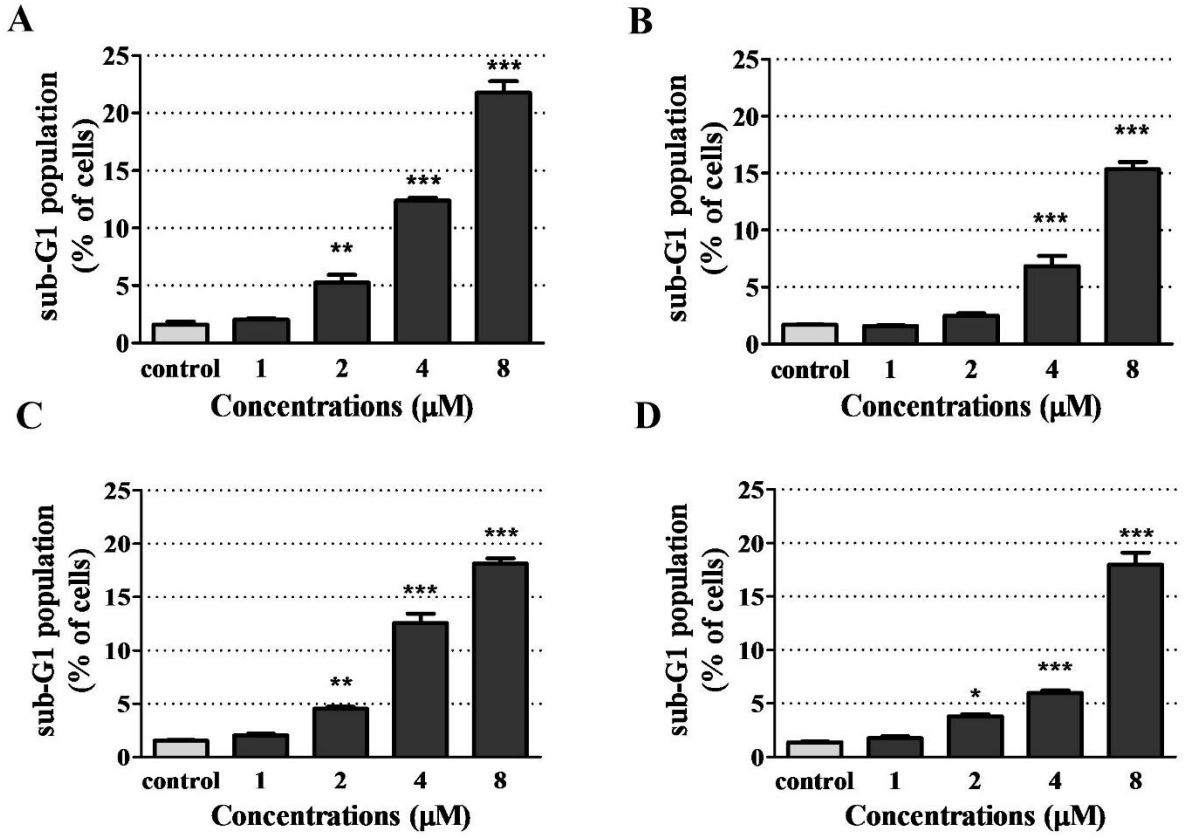

Figure 7. Compound **1** caused significant and concentration-dependent elevation in proportion of hypodyploid sub-G1 phase. As a sign of programmed cell death, sub-G1 fractions were determined after 48 h treatment in MCF-7 (A) and MDA-MB-231 (B) breast cancer cells and SiHa (C) and C33A (D) cells derived from malignant human cervical tissue. *, ** and *** indicate $p<0.05$, $p<0.01$ and $p<0.001$ respectively, compared to the untreated cells.

Besides these findings, significant accumulation of cells in G2/M phase to the detriment of G0/G1 phase were observed in all examined malignant cell lines (**Figure 8**). In case of MDA-

MB-231 cells – due to their lesser sensitivity against the test substance – experiments were repeated after 72 h incubation with compound **1**, while on other cell lines, cell cycle analyses were accomplished 48 h post-treatment.

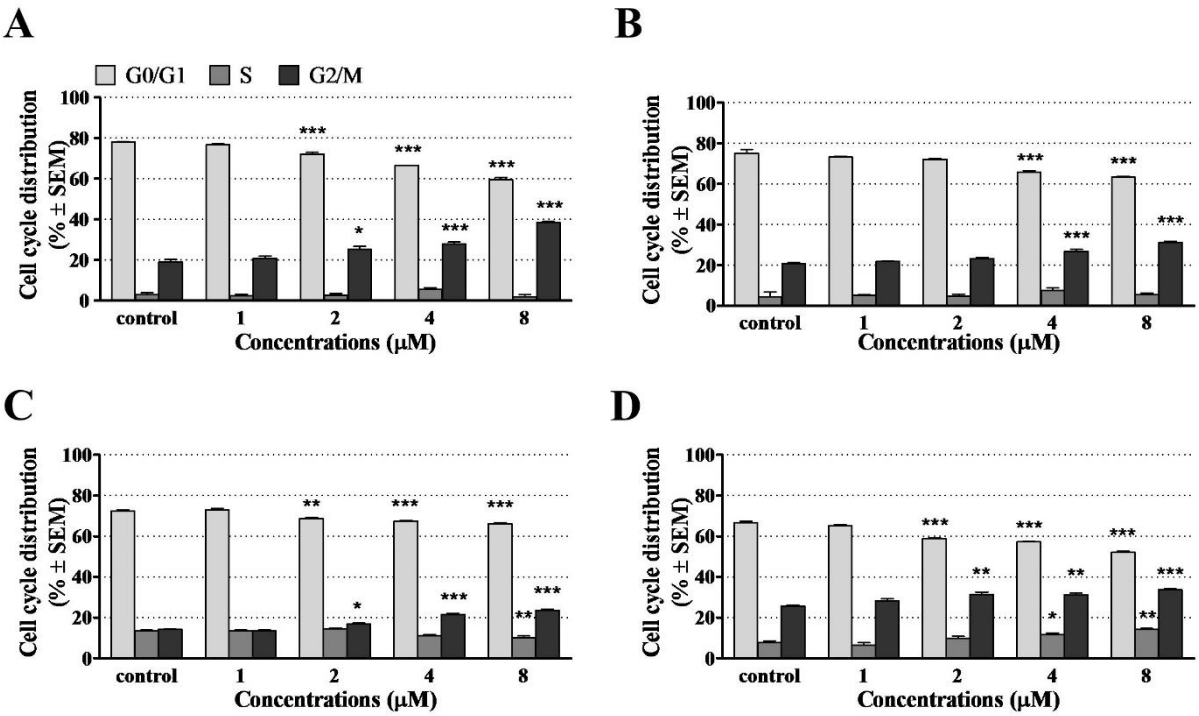

Figure 8. Test compound **1** induced cell cycle disturbances via accumulation of cells in the G2/M phase and reduction of the G0/G1 phase. Experiments were carried out on MCF-7 (A), SiHa (C) and C33A (D) cell lines 48 h post-treatment, while in the case of triple negative breast cancer cell line (B), 72 h incubation time showed favourable effect. *, ** and *** indicate $p<0.05$, $p<0.01$ and $p<0.001$ respectively, compared to the untreated control.

4.5 Determination of caspase-3 activity

The significant, concentration-dependent increase in the ratio of sub-G1 phase, regarded as the apoptotic cell fraction during cell cycle analysis, clearly demonstrated the ability of the tested compound to induce programmed cell death (**Figure 9**). To further confirm this phenomenon, changes in the activity of major executive proapoptotic enzyme, caspase-3, were quantified. The androstadiene analogue, compound **1** enhanced the caspase-3 activity by 1.6 to 2.6-fold after 24, 48 and 72h exposure at ≥2 μM concentrations on the SiHa cell line.

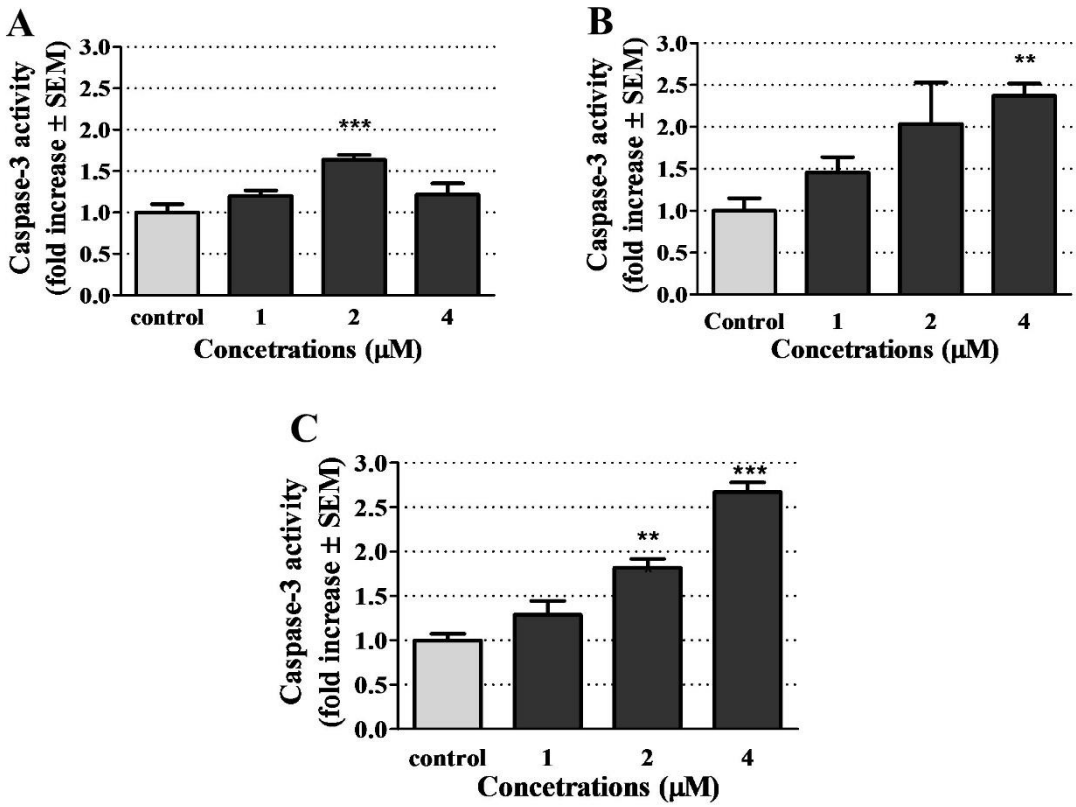

Figure 9. During colorimetric determination, caspase-3 activity was elevated after compound **1** treatment. Time and concentration-dependent changes in enzymatic activity were detected in SiHa cells 24 h (A), 48 h (B) and 72 h (C) post-treatment. ** and *** represent $p<0.01$ and $p<0.001$ respectively, compared to the untreated control.

4.6 Mitochondrial membrane potential assay (JC-1 staining)

Origin of the induced programmed cell death, revealed by fluorescent double staining, cell cycle analysis and caspase-3 assay earlier, was determined by mitochondrial membrane potential assay. In MCF-7, MDA-MB-231, SiHa and C33A samples stained by JC-1 dye, a concentration-dependent elevation in the percentage of subpopulations emitting green fluorescence were detected (**Figure 10**). In case of the MCF-7 and MDA-MB-231 cell lines, ratios of cells with depolarized mitochondrial membranes significantly increased by 16% and 4%, respectively, at the highest applied concentration compared to untreated cells 12 h post-treatment. In case of SiHa and C33A cells, pronounced elevation in proportion of cells with disrupted mitochondrial membrane potential was recorded after 24 h of treatment at the same concentration (numerically, increased by approximately 46% in SiHa and by 35% in C33A cells).

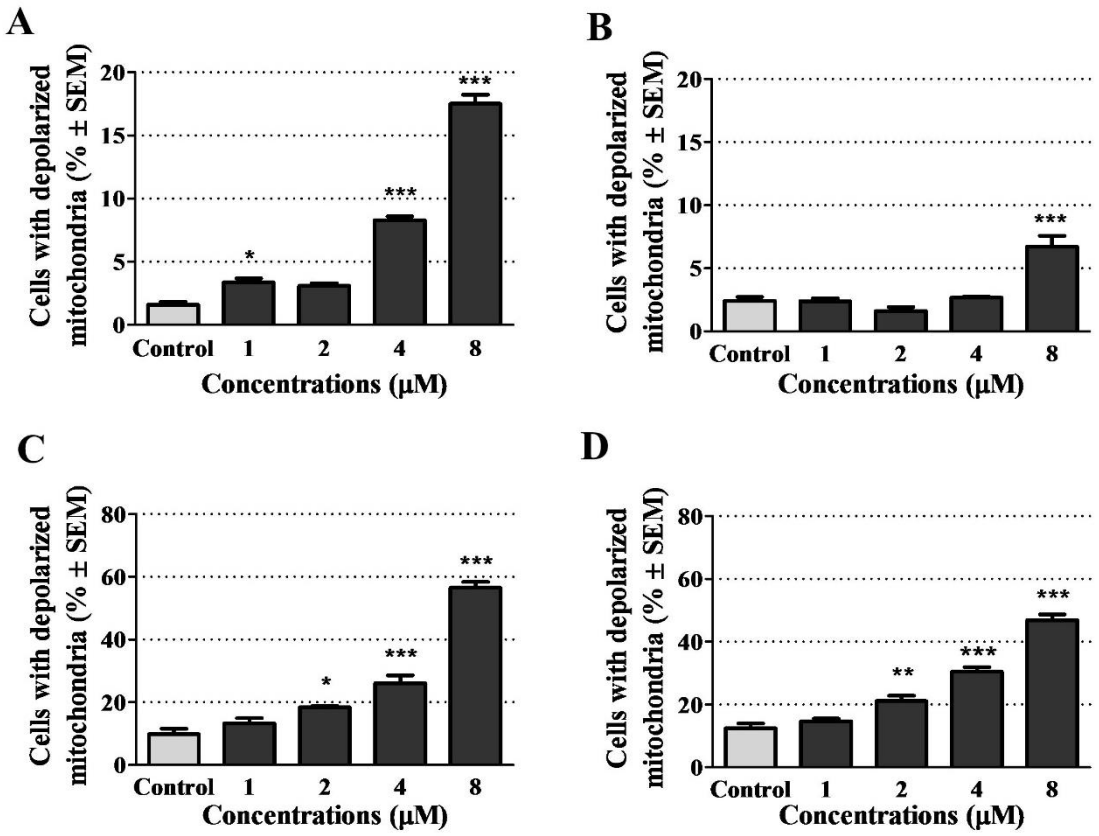

Figure 10. Compound **1** generated disturbances of mitochondrial membrane potential in breast and cervical cancer cell lines. Considerable, concentration-dependent alterations in mitochondrial membrane integrity were observed in MCF-7 (A) and MDA-MB-231 cells (B) 12 h post-treatment and in SiHa (C) and C33A cells (D) after 24 h incubation with the test substance. *, ** and *** represent $p<0.05$, $p<0.01$ and $p<0.001$ respectively, compared to the control.

4.7 Yeast androgen screen assay (YAS)

To confirm the hypothesized mechanism of action, which corresponds to antitumor activity without a hormonal background based on previous structure-activity relationships and literature data, the YAS assay was performed. In the presence of an androgen-sensitive, genetically modified yeast strain (*S. cerevisiae*), no substantial androgenic or antiandrogenic activity of compound **1** were identified compared to 5α-dihydrotestosterone (DHT) in the agonistic and to flutamide in antagonistic determination, used as reference agents after 48 h exposure (**Figure 11**).

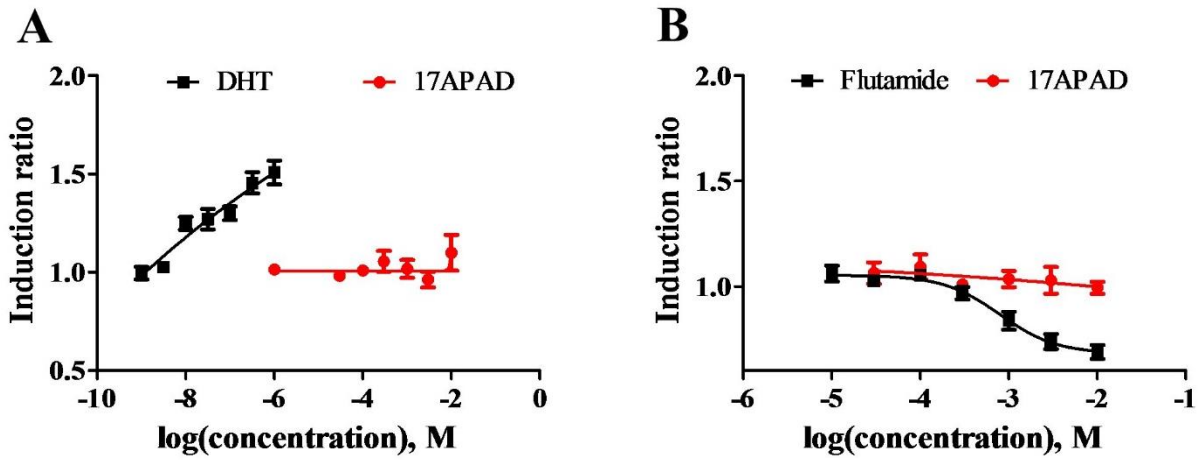

Figure 11. Compound **1** exerted no substantial agonistic or antagonistic activity on androgenic receptor in YAS assay. The hormonal potential was determined compared to DHT (A) and antihormonal effects were examined in the presence of DHT compared antiandrogenic activity of flutamide used as a reference agent (B) on a genetically modified *S. cerevisiae* strain 48 h post-treatment.

4.8 Wound-healing assay

To characterize the antimetastatic profile of compound **1**, inhibition of collective cell migration as one of the main hallmarks of metastatis formation, was quantified. Alterations in the cell migratory capacity in response to experimental application of sub-antiproliferative concentrations of the test compound were assessed by wound-healing assay.

Image analysis confirmed noteworthy decrease in migratory capacity of MCF-7 cells by 30.8% and 22.8% at 0.3 μM compared to control after 24 or 48 h treatment (**Figure 12**). Similarly, influence of compound **1** to migration of SiHa cells manifested in a significant reduction of wound-closure by 9.0% and 21.7% at 0.03 μM 24 h or 48 h post-treatment, respectively.

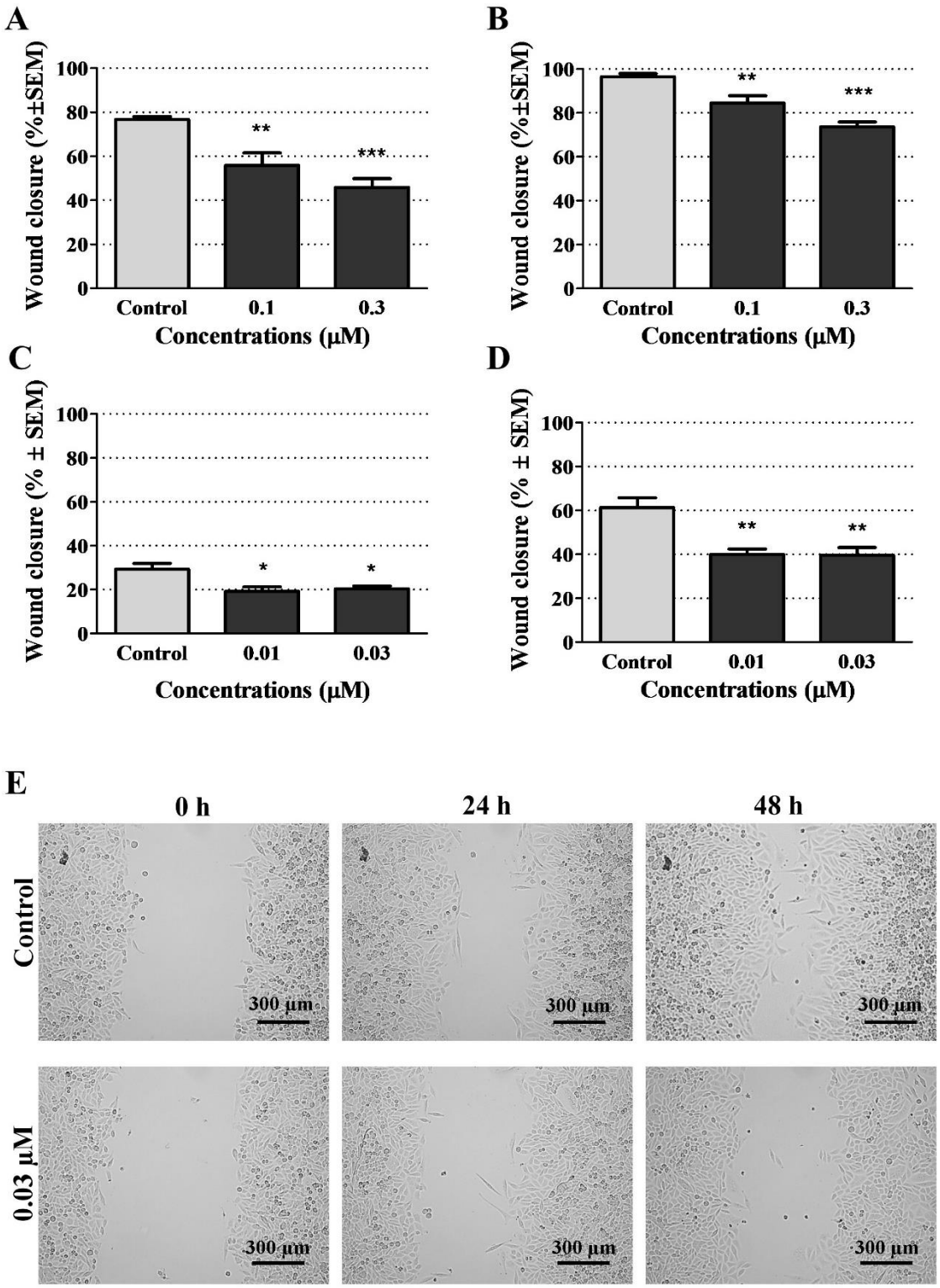

Figure 12. Compound **1** significantly reduced the migrative capacity of breast and cervical cancer cells. Rates of wound closure in MCF-7 (A, B) and SiHa (C, D) samples expressed in percentage were greatly decelerated after exposed to low concentrations of the test substance for 24 h (A, C) or 48 h (B, D).

Representative images of SiHa cells from 0, 24 and 48 h of treatment (E). *, ** and *** indicate $p<0.05$, $p<0.01$ and $p<0.001$ respectively, compared to the control.

4.9 Boyden chamber assay

As a model of cell invasion via the basement membrane, special inserts containing matrigel membrane pre-coated with extracellular matrix proteins mimicking the environment of primary tumor, were used. In this system, the number of invading MDA-MB-231 triple negative breast cancer cells were decreased by approximately 70% at 0.3 μM (**Figure 13**). Furthermore, number of invading cervical SiHa cells were significantly diminished by 48.9% after application of 0.03 μM of compound **1** for 24 h.

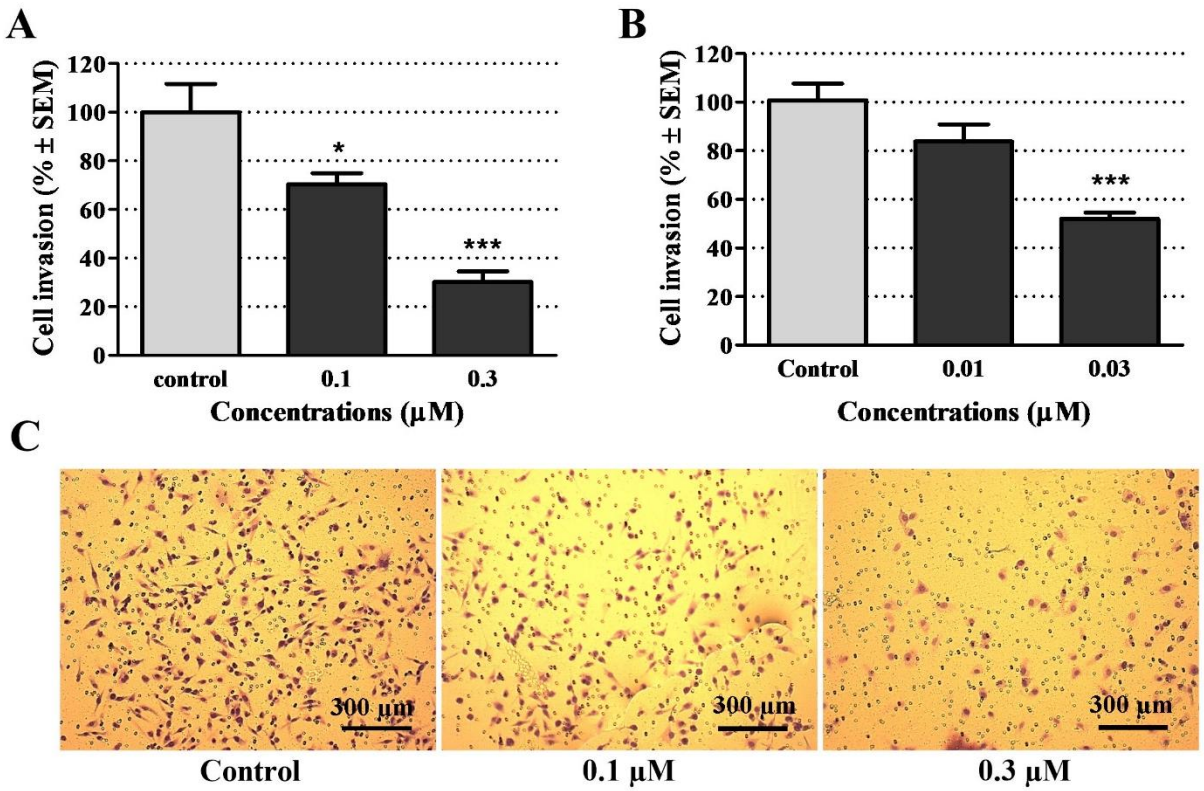

Figure 13. Compound **1** significantly reduced the invasivness of triple negative breast cancer cells and HPV-16 positive cervical cancer cells. Anti-invasive properties of the test substance were demonstrated by considerable decrease in percentage of invading MDA-MB-231 (A) and SiHa (B) cells in the treated samples compared to untreated control and representative images about MDA-MB-231 cells 24 h post-treatment (C). Data indicate mean ± SEM. * and *** represent $p<0.05$ and $p<0.001$ respectively.

4.10 CCIDs assay

To assess the effects on intravasation rate, the CCIDs assay as a 3D model of biochemical interactions between malignant cells and lymphendotelial monolayer were accomplished after short-term incubation with the test substance. Accordingly, cancer spheroids – consisting of MCF-7 cells – induced gap-formation in the monolayer of iLEC cells; this process was significantly inhibited by treatment with compound **1** or defactinib, which served as positive control (**Figure 14**). These findings were evidenced by a decrease in size of cell-free areas underneath the tumor spheroids in a concentration-dependent manner at ≥2 μM, which were comparable with the effect of defactinib, a potent focal adhesion kinase (FAK) inhibitor agent. However, the structurally-similar epiandrosterone, only exerted a minor anti-invasive effect at 40 μM.

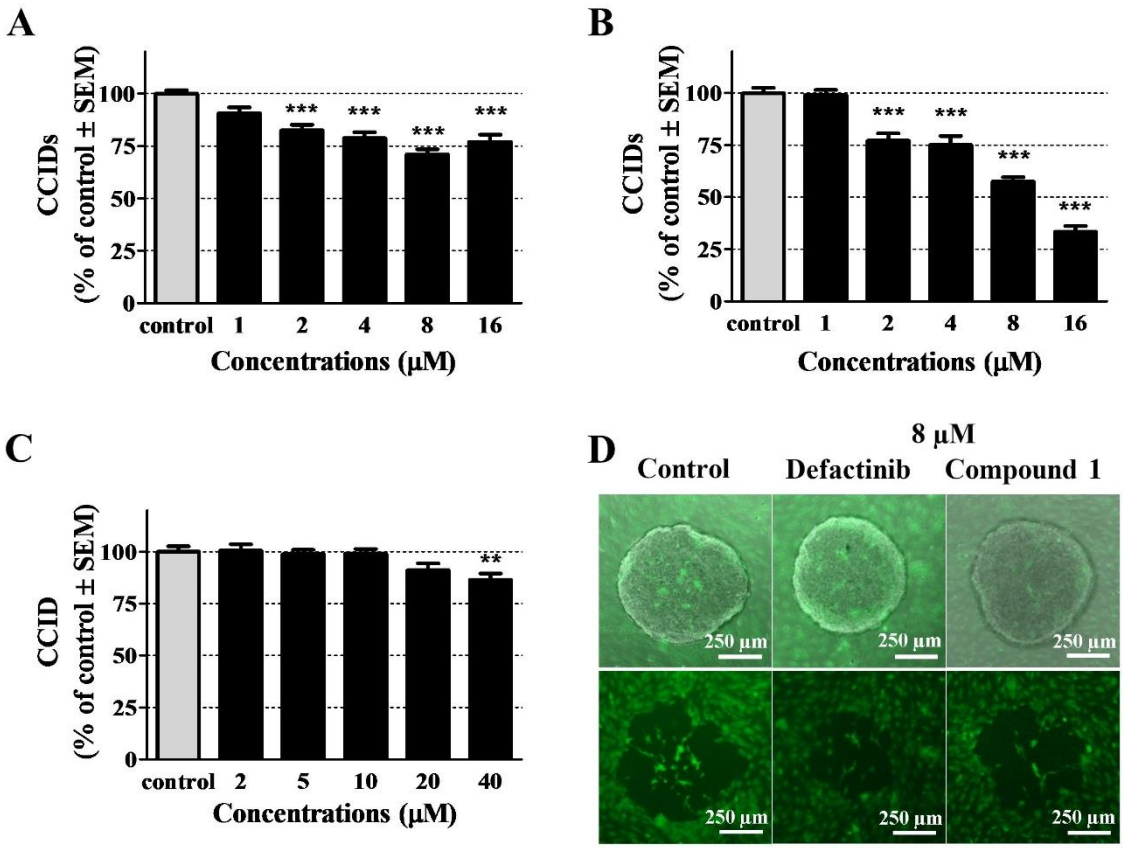

Figure 14. Compound **1** exerted an anti-invasive characteristic comparable with defactinibe, a potent FAK inhibitor (D, representative images of cancer spheroids and cytotracker-stained endothelial monolayer). Our test substance (A) and defactinib (B) decreased size of cell-free areas at 2 μM 4 h post-treatment, while structurally related epiandrosterone (C) showed significant anti-invasive effect at 20-

fold higher concentration only on MCF-7/iLEC model. ** and *** indicate $p<0.01$ and $p<0.001$ respectively, compared to the control.

4.11 Single cell mass cytometry

To characterize the tumor marker profile of chemosensitive subpopulations of the MDA-MB-231 cell line, nine carcinoma markers were investigated at single cell resolution. The multidimensional analysis, the visualization of t-distributed stochastic neighbour embedding (viSNE) demonstrated the clonal heterogeneity of single-cell effects induced by compound **1,** based on the area of viSNE plots. The colour shifts of single cells recorded after 72 h of treatment are proportional to the expression level of the examined carcinoma markers, characterizing the various subpopulations of MDA-MB-231 cells (**Figure 15/A**). Substantial decrease was detected in the percentage of cells positive for EGFR, CD274 (PD-L1), and CD326 (EpCAM) within the drug-sensitive population upon the treatment of compound **1**, as determined by manual gating. On the other hand, elevated expression levels of GLUT1, MCT4, Pan-Keratin, CD66 (a,c,e), Gelactin-3 and TMEM45A were observed in the chemosensitive populations(**Figure 15/B**).

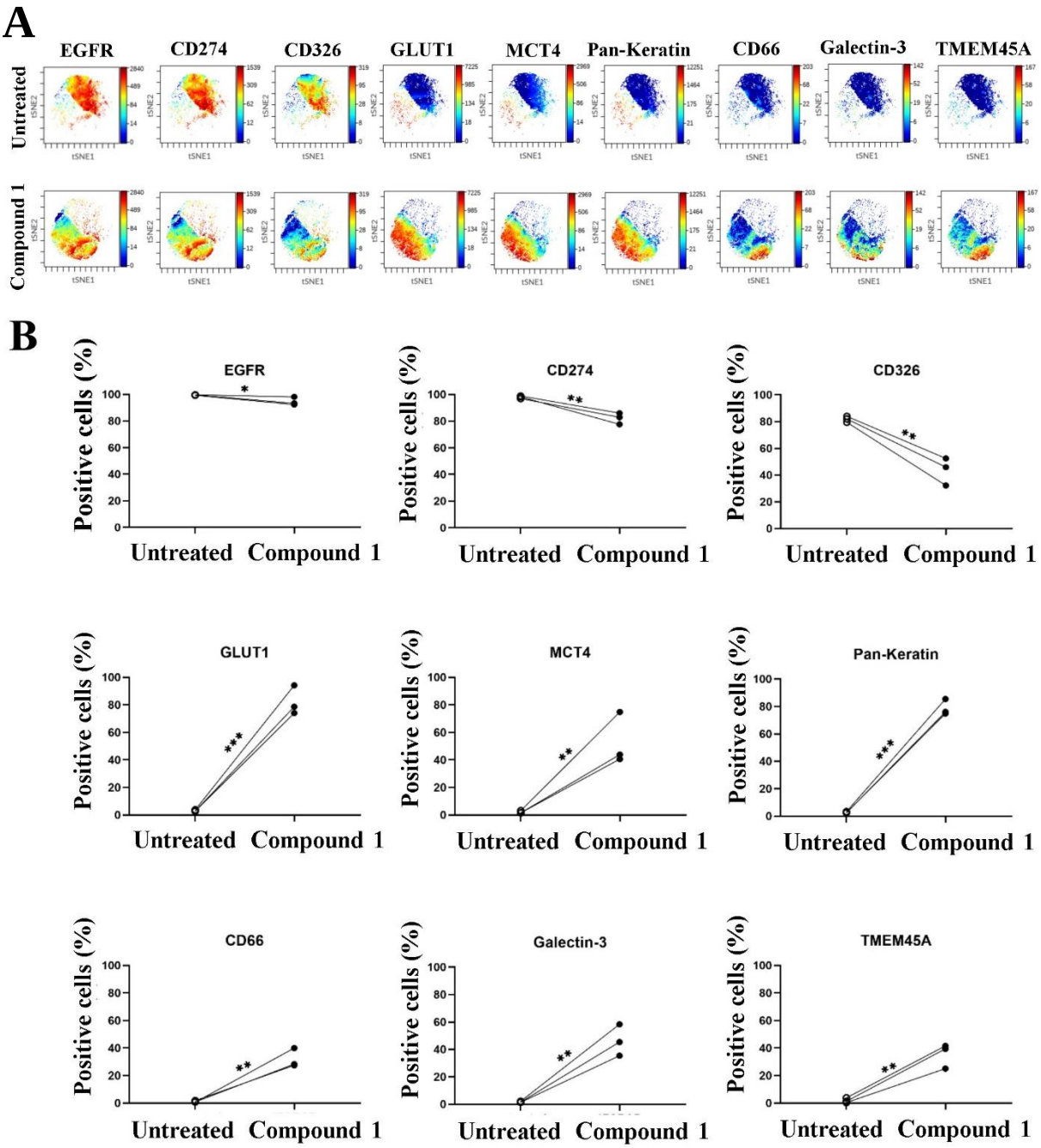

Figure 15. Representative multidimensional visualization at single cell resolution of changes in the levels of 9 carcinoma marker proteins, induced by compound **1** in the MDA-MB-231 cell line (A). After the 72 h incubation with 8 μM of compound **1**, the percentage of cells positive for EGFR, CD274 and CD326 reduced and the percentage of cells positive for GLUT1, MCT4, Pan-Keratin, CD66(a,c,e), Galectin-3, TMEM-45A elevated in the chemosensitive subpopulation (B). *, ** and *** indicate $p<0.05$, $p<0.01$ and $p<0.001$, respectively, compared to control.

4.12 *In vivo* mouse breast cancer model

The 4T1 mouse breast cancer model as an appropiate *in vivo* model of highly invasive, advanced stage human breast cancer was selected to prove the antitumoral effect of compound **1**. After 2 weeks of intraperitoneal administration of 25 mg/kg dose, a significant reduction in weight of the induced tumor tissues (control group: 971.8 ± 82.56 mg and treated group: 504.1 ± 76.56 mg) was observed (**Figure 16**). In addition, noteworthy deceleration in tumor growth rate was revealed in the treated group from the fourth day of the application period, compared to the control animals without provoking of severe, life-threatening side effects.

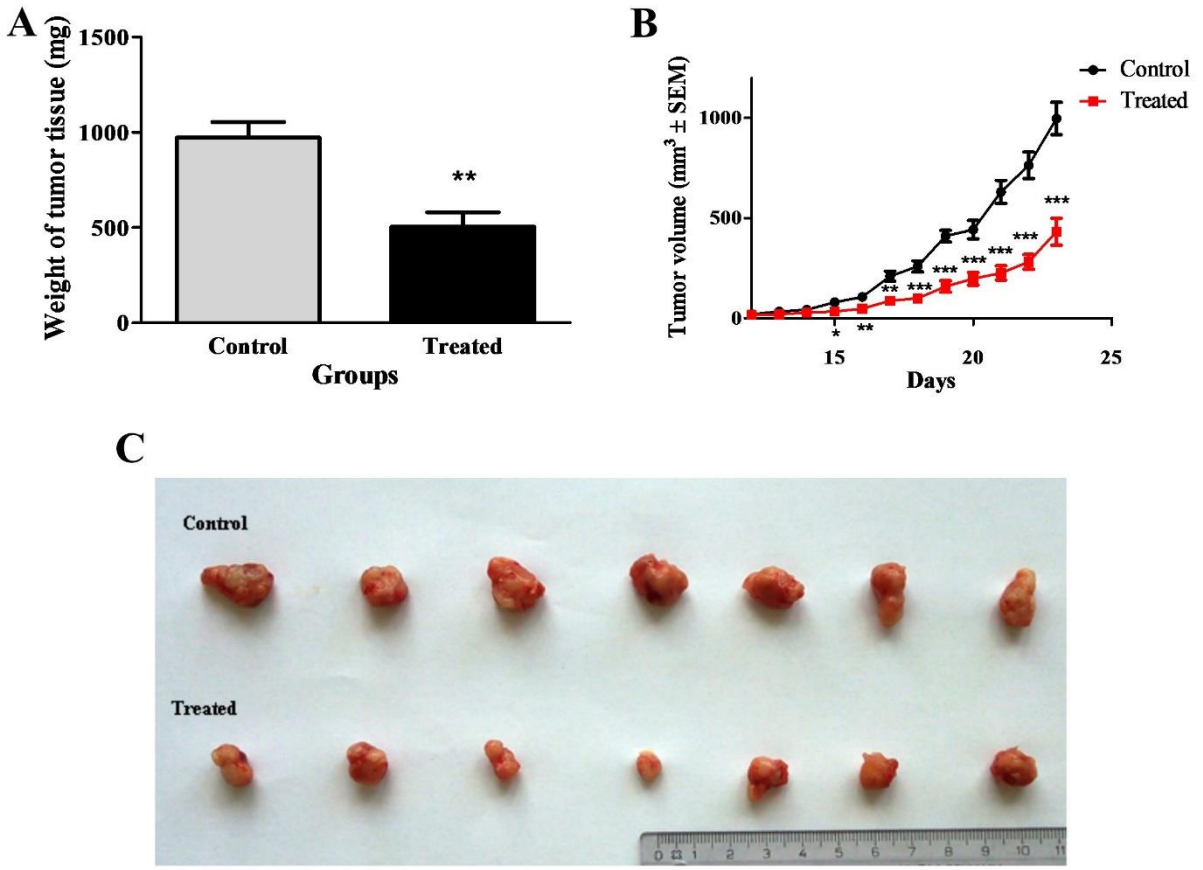

Figure 16. Tumor growth rate significantly reduced after treatment with compound **1**. After 14 days of intraperitoneal application, the mean weight of surgically removed tumor tissues (n=7) were considerable decreased in the experimental group (A, C). Tumor growth curves (B) demonstrate a significant growth inhibitory effect of compound **1** *in vivo*. *, ** and *** indicate $p<0.05$, $p<0.01$ and $p<0.001$ respectively, compared to the control.

5 DISCUSSION

Natural steroids, such as cholesterol, ergosterol, different types of fitosterols or human steroidal hormones are all essential facilitators in several biological processes. In the human body, sexual steroids exhibit great impact on cell proliferation, but precisely because of this, they may also be responsible for the development and progression of several hormone-dependent malignancies, such as breast or prostate cancer. On the other hand, modification of their structure at relevant positions, especially on the A- and/or D-ring, may yield novel anticancer agents, preserving favorable pharmacological and pharmacokinetic properties of the steroid skeleton.[39] Some of these derivatives are already an integral part of antitumoral therapy (e.g., abiraterone) or are currently undergoing evaluation in clinical trials (e.g., galeterone). Accordingly, many steroid analogues used in this and other therapeutic fields have a common property, i.e. they are generally substituted at the C-17 position of the D-ring with an *exo*-heterocyclic ring, which alters the binding affinity of the compound to the receptors and other cellular compartments, and their spectrum of biological activity.[60] Numerous studies of structure-activity relationships have confirmed considerable changes in biological properties after incorporation of various substituents, including heteroaromatic rings at C-17 position.[43,61,62] From these semisynthetic analogues, androstane derivatives are less studied chemical entities than their counterparts from the estrange series, but their favourable anticancer effects were highlighted by several studies. Thiazolo-androstenone derivatives synthesized by Ali *et al*., exerted pronounced antiproliferative activity against five leukaemia, two non-small cell lung cancer, four colon cancer, four central nervous system cancer, five melanoma, two ovarian cancer, six renal cancer, two prostate cancer and three breast cancer cell lines from the cancer panel of National Cancer Institute (NCI), containing 60 cell lines.[63] Another promising library of steroids from the androstane and estrane series, bearing pyrimidine- and dihydrotriazine moiety were reported by Scherbakov *et al.* and their lead molecule showed high selectivity towards the MCF-7 breast cancer cell line.[49] Novel isatin conjugates, derived from epiandrosterone or androsterone with antineoplastic potential were tested against gastric cancer (SGC-7901), melanoma (A875) and hepatocellular liver carcinoma (HepG2) cell lines, in a report published by Ke and co-workers.[64] Furthermore, our previous works demonstrated antitumoral properties of D-ring modified androstane derivatives as well. Among others,

outstanding antiproliferative influence of novel 17α-halogenic 19-nortestosterone analogues, 17β-pyrazol-5'-ones in the Δ5-androstane series and 17-5′-(1′,2′,4′)-oxadiazolyl androstenes were demonstrated against human breast and gynaecological cancer cell lines in our studies earlier.[51,65,66] Based on these facts, our previous results and literature data, D-ring substituted or fused androstane analogs containing a heterocyclic ring of pyrazole, triazole or tetrazole were designed and synthesized as reported earlier.[51,65,66]

The aim of the present study was to evaluate the pharmacological potential of four D-ring modified androstane derivatives, with special regard to their antiproliferative and antimetastatic properties on breast and gynaecological cancer cells.

Out of the four compounds described above, only compound **1** exerted considerable growth inhibition after 72 h of treatment in a standard MTT assay. The antiproliferative effect of compound **2**, **3** and **4** did not reach the threshold of at least 50% of inhibition at 30 μM concetration in most of the cases. IC_{50} values of the candidate compound (**1**) were lower than 2 μM on cervical and breast cancer cell lines, which exhibits at least a two-fold increase in sensitivity, compared to the impact of therapeutically-applied cisplatin used as a reference agent. These results are also comparable to the structurally-related molecules and abiraterone presented earlier, therefore, this compound was selected as the focus of our further studies.[55,67,68]

Tumor selectivity is one of the most important criterias for safe administration of antineoplastic drugs. Accordingly, antiproliferative analysis of our test substance was extended to non-cancerous fibroblast cells as well. Tumor selectivity indices of compound **1** calculated as described above, were ranged from 0.2 to 0.7; in contrast, indices of cisplatin presented with an absolute lack of selectivity, which manifested in higher values than 1.1 on cervical and breast cancer cells.

In order to identify the causative factors of inhibition upon cell proliferation, morphological signs of programmed cell death were examined by fluorescent double staining methods. Chromatin condensation in early apoptotic cells and loss of membrane integrity in necrotic and secondary necrotic cells were visualised under a fluorescent microscope by Hoechst33258/PI staining after 24 h incubation with the test substance, which indicated a significant increase in apoptotic and necrotic cell population as well in MCF-7 and SiHa samples. To resolve limitations of this microscopic method, and for an even more detailed

separation of different cell fraction such as early vs. late apoptotic and necrotic cells, Annexin V-Alexa488/PI fluorescent double staining were performed by flow cytometry. Significantly elevated subpopulations of late apoptotic (AnnV+/PI+) cells were detectable at ≥2 μM without greater accumulation of necrotic (AnnV–/PI+) cells on all of the utilized cell lines. In addition, a proapoptotic characteristic was confirmed by the elevated proportion of sub-G1 subpopulation in the cell cycle analysis on the utilized four malignant cell lines (MCF-7, MDA-MB-231, C33A, SiHa) as well. In our previous studies, D-ring-modified androstane derivatives typically induced significant cell cycle disruptions after 48 h of treatment, so our experiments were performed after 48 or 72 h incubation when it was necessary.[46,51] In all cases, a considerable arrest and accumulation of cells in the G2/M phase were observed in the expense of cells in the G0/G1 phase, accompanied by noteworthy, concentration-dependent elevation in the proportion of hypodiploid sub-G1 fractions regarded as the natural outcome of apoptosis.

Nevertheless, the development of morphological changes during apoptosis may be traced back to multistep protein-protein interactions, including activation of the caspase cascade. A major enzyme of the execution phase, responsible for chromatin condensation and DNA fragmentation, is caspase-3; the activity of this enzyme was elevated to more than 1.5-fold after 24, 48 and 72 h exposure to 2 μM of compound **1**. Although, the caspase-3 enzyme may be activated during both the intrinsic and the extrinsic pathway of apoptosis, JC-1 staining indicated a disruption of mitochondrial membrane potential and integrity after 12 hours of exposure on breast carcinoma cell lines and after 24 h of treatment on cervical cell lines, corroborating the intrinsic origin of apoptosis.

Stuctures of nuclear hormone receptors are very conservative, with 12 helices forming a hydrophobic pocket in their ligand-binding region, where ligands make different contacts with amino-acid residues, promoting conformational changes. In addition, for the activation of androgen receptors, hydrophobic interactions or hydrogen bonding between the 3-keto group and side chains of residues Q711 and R752, as well as between the 17β-OH group and side chains of N705 and T877 – or moieties mimicking these bonds – are crucial.[40,69] If new chemicals without hormonal activity would be synthesized, then these structural requirements should be avoided. Based on previous results and structure-activity relationships, we hypothesize that a bulky steric structure such as the 1'-4"-cyanophenyl-4'-hydroxymethyl-1'H-pyrazol-3'-yl moiety at position C-17 of the androstadiene skeleton, may diminish or prevent

binding of the test compound to the androgen receptor. Lack of androgen activity have been confirmed by YAS assay on a genetically modified *S. cerevisiae* strain. Androgenic and antiandrogenic activity of our test substance was found to be negligible, compared to the effect of reference agents, DHT and flutamide.

According to several epidemiological and clinical surveys, a remarkable proportion of cancer-related deaths can be attributed to metastasis formation.[70,71] For example, the examined MDA-MB-361 human breast cancer cell line is derived from a brain metastasis. For a long time, 17β-estradiol has been known to stimulate proliferation of malignant tissues and cells; conversely, the androgen hypothesis, explains the role of testosterone and its active metabolite, 5α-dihydrotestosterone, in the progression of prostate cancer and the subsequent spread of the primary tumor cells to distant organs. However, nowadays more and more contradictory studies are being published about the effects of androgens on metastasis formation and progression. While in some studies, testosterone did not increase the size of metastases *in vivo*, even going so far as having it accepted in protocols for the treatment of metastatic breast cancer more than four decades ago. Other studies suggested that androgens, via their nuclear receptor, induce genomic binding to estrogen receptors and regulate the transcription of genes that promote breast cancer cell proliferation, motility, invasion, and survival; therefore, progression of estrogen receptor positive breast cancer may be improved by antiandrogen administration.[36,72,73] As metastasis formation is highly associated with poor prognosis of patients, the prevention or inhibition of this multistep process is crucial in the future of tumor therapy. In the first stage of metastasis progression, the migration of cancer cells to neighbouring tissues and the invasion through the basement membrane occurs. In the *in vitro* experimental systems, the drug candidate (**1**) significantly inhibited migration of SiHa and MCF-7 cells and invasion of highly invasive MDA-MB-231 and SiHa cells at sub-antiproliferative, nanomolar concentrations even after 24 h of treatment. Migrated cells have to enter the circulatory system by intravasation into the lymphatic system or blood vessels. During intravasation, cancer cells or cell aggregates interact with the endothelial barrier and induce a gap formation on it via different biochemical reactions and signal transduction pathways.[74] In a 3D, co-culture CCIDs assay, compound **1** reduced the size of cell free-areas on a lymphatic endothelial monolayer underneath the MCF-7 tumor emboli by 30% after 4 h of treatment at 8 μM and showed comparable inhibition to defactinib, a potent FAK-inhibitor at lower concentrations. These values are more pronounced

than inhibition by epiandrosterone, a structural analogue, in the same system. Epiandrosterone is known as an L-type Ca^{2+}-channel inhibitor, which effect was demonstrated in similar experimental system, where this substance reduced the elevated intracellular Ca^{2+} levels induced by 12(S)-HETE.[75] Therefore, the antimetastatic mechanism of action of our test compound (**1**) is presumably related to other or additional reactions than the inhibition of Ca^{2+}-channels alone, which require further investigations.

Expression level of cell surface markers such as EGFR, CD274 or CD326, associated with the malignant characteristic of solid tumors, may carry important data about the chemosensitivity of the cells and their mechanisms of adaptation upon a treatment.[76–78] Treatment with compound **1** decreased the expression of EGFR, CD274, and CD326 in the sensitive subpopulations of MDA-MB-231 cells, while increased level of GLUT1, MCT4 Pan-Keratins (the clone C11 antibody detects keratins: 4, 5, 6, 8, 10, 13 and 18), CD66, Gal-3, and TMEM45A were observed. These data probably indicate the increased chemosensitivity and the metabolic reprogramming of cells as a compensatory mechanism, activated upon the test substance-induced oxidative stress.[79–84] Interestingly, the population of CD66(a,c,e)-positive cells showed overlapping with the TMEM45A-positive cells.

Finally, exceeding the possibilities offered by *in vitro* methods, antitumor properties of the examined androstadiene derivative (**1**) were tested on the 4T1 breast cancer model, induced in mammary pad of BALB/c mice.[85,86] This *in vivo* model is corresponded to advanced stage, highly invasive, triple-negative human breast cancer. After 2 weeks of intraperitoneal administration, size of developing tumors were approximately 50% relative to control samples without severe, life-threatening side effects.

In conclusion, our experimental data revealed favorable antiproliferative and antimetastatic characteristics of 3β-hydroxy-17-[1’-(4’’-cyanophenyl)-4’-hydroxymethyl-1’H-pyrazol-3’-yl]androsta-5,16-diene, while D-ring fused triazole and tetrazol derivatives did not exert similar properties. Proapoptotic properties via activation of the intrinsic pathway with moderate tumor selectivity and potent antimigratory, anti-invasive and anti-intravasative effects, without hormonal potential have been identified as part of the mechanism of action. In the light of these results, substituation of androsta-5,16-diene framework at C-17 position with heterocyclic moieties containing nitrogen atoms should be considered for the design and synthesis of novel, effective antitumor agents.

6 SUMMARY

In conclusion, the principal results of our experiments are the following:

- From the four examined novel androstane derivatives, compound **1** exerted pronounced antiproliferative properties on breast and gynecological malignant cell lines (HeLa, SiHA, C33A, A2780, MCF-7, T47D, MDA-MB-231, MDA-MB-361). Calculated IC_{50} values were lower than 2 μM on the investigated cervical and breast cancer cell lines.
- Tumor selectivity indices were between 0.2 and 0.7, which represent moderate tumor selectivity.
- Fluorescent double staining, carried out by fluorescent microscopy and flow cytometry, highlighted the proapoptotic properties of compound **1**, which were confirmed by elevated sub-G1 cell population in cell cycle analysis and increased caspase-3 activity. Mitochondrial origin of programmed cell death was identified by JC-1 staining.
- Becuse of D-ring modified androstane skeleton, hormonal activity of the tested substance was investigated on an androgen sensitive, genetically modified *S. cerevisiae* strain. Compund **1** did not indicate any androgenic or antiandrogenic potential, compared to 5α-dihydrotestosterone or flutamide used as reference agents.
- Antimetastatic characteristic of our test substance was demonstrated by inhibiting of cell migration, invasion and intravasation at sub-antiproliferative concentrations in 2D and 3D *in vitro* assays (wound-healing, Boyden chamber, CCIDs).
- As a possible sign of increased chemosensitivity and metabolic reprogramming of the sensitive subpopulations of MDA-MB-231 cells upon treatment with compound **1**, changed expression level of nine cell surface markers were observed.
- Application of compound **1** in ortothopic 4T1 mouse mammary tumor model, which is an *in vivo* reproduction of clinically-relevant triple negative human breast cancer, caused a significant reduction in the size of induced primary tumors.

In summary, the examined D-ring modified androstadiene analogue, containing pyrazole substituent at position C17, exerted potent aniproliferative and antimetastatic

properties on breast and gynaecological cancer cell lines *in vitro* and *in vivo*; therefore, it should be considered as a prototype for the design of novel, promising anticancer steroidal agents without hormonal activity.

7 GLOSSARY OF ACRONYMS AND ABBREVIATIONS

- **12(S)-HETE:** 12S-hydroxy-5Z,8Z,10E,14Z-eicosatetraenoic acid
- **ANOVA:** analysis of variance
- **ATCC:** American Type Culture Collection
- **BALB/c:** albino, laboratory-bred strain of the house mouse
- **Bcl-2:** B-cell lymphoma 2 protein
- **BRC1/BRC2:** breast cancer type 1 susceptibility protein gene / breast cancer type 2 susceptibility protein gene
- **CCIDs:** circular chemorepellent-induced defects assay
- **CD274/PD-L1:** cluster of differentiation 274 / programmed death-ligand 1
- **CD326/EpCAM:** cluster of differentiation 326 / epithelial cell adhesion molecule
- **CD66(a,c,e):** carcinoembryonic antigen-related cell adhesion molecules
- **CO_2:** carbon dioxide
- **CPRG:** chlorophenol red-β-D-galactopyranoside
- **CYP17A1:** steroid 17α-hydroxylase/17,20 lyase
- **DHT:** 5α-dihydrotestosterone
- **DMSO:** dimethyl sulfoxide
- **DNA:** deoxyribonucleic acid
- **ECACC:** European Collection of Authenticated Cell Cultures
- **EGM-2MV:** Microvascular Endothelial Cell Growth Medium-2
- **EMEM:** Eagle's Minimum Essential Medium
- **EphA2:** ephrin type-A receptor 2
- **FAK:** focal adhesion kinase
- **FBS:** fetal bovine serum
- **G1:** first growth phase in cell cycle
- **G2/M:** second growth phase in cell cycle with double DNA content / mitotic phase
- **Gal-3:** Galectin-3
- **GLOBOCAN:** Global Cancer Observatory
- **GLUT1:** glucose transporter 1

- **HEPA:** high-efficiency particulate absorbing filter
- **HEPES:** 2-[4-(2-Hydroxyethyl)-1-piperazinyl]-ethanesulfonic acid
- **HPV:** human papillomavirus
- **HER2:** human epidermal growth factor receptor 2
- **IARC:** International Agency for Research on Cancer
- **IC_{50}:** half maximal inhibitory concentration
- **IVC:** individually ventilated cage
- **JC-1:** 5,5',6,6'-tetrachloro-1,1',3,3'-tetraethyl-benzimidazolylcarbocyanine iodide, fluorescent dye
- **L-15:** Leibovitz's L-15 medium, designed to be used for cell cultures without additional CO_2 in their atmosphere
- **Mcl-1:** induced myeloid leukemia cell differentiation protein
- **MCSB:** Maxpar Cell Staining Buffer
- **MCT4:** monocarboxylate transporter 4
- **MTT:** 3-(4,5-dimethylthiazol-2-yl)-2,5-diphenyltetrazolium bromide
- **p:** p-value, level of statistical significance
- **p53:** cellular tumor antigen p53
- **PBS:** phosphate buffer solution
- **PET:** polyethylene terephthalate
- **RPMI:** Roswell Park Memorial Institute medium
- **S:** phase of DNA replication
- **SEM:** standard error of the mean
- **Src:** proto-oncogene tyrosine-protein kinase Src, non-receptor tyrosine kinase protein
- **Sub-G1:** hypodiploid cell fraction
- **TMEM45A:** transmembrane protein 45A
- **WHO:** World Health Organization
- **YAS:** yeast androgen screen assay

8 REFERENCES

1. Sung, H. *et al.* Global cancer statistics 2020: GLOBOCAN estimates of incidence and mortality worldwide for 36 cancers in 185 countries. *CA. Cancer J. Clin.* **71**, 209–249 (2021).
2. DeVita, V. T. & Chu, E. A history of cancer chemotherapy. *Cancer Res.* **68**, 8643–8653 (2008).
3. Bray, F. *et al.* Global cancer statistics 2018: GLOBOCAN estimates of incidence and mortality worldwide for 36 cancers in 185 countries. *CA. Cancer J. Clin.* **68**, 394–424 (2018).
4. Ferlay, J. *et al.* Cancer incidence and mortality worldwide: Sources, methods and major patterns in GLOBOCAN 2012: Globocan 2012. *Int. J. Cancer* **136**, E359–E386 (2015).
5. Ferlay, J. *et al.* Estimates of worldwide burden of cancer in 2008: GLOBOCAN 2008. *Int. J. Cancer* **127**, 2893–2917 (2010).
6. Parkin, D. M., Bray, F., Ferlay, J. & Pisani, P. Global cancer statistics, 2002. *CA. Cancer J. Clin.* **55**, 74–108 (2005).
7. Parkin, D. M., Bray, F., Ferlay, J. & Pisani, P. Estimating the world cancer burden: Globocan 2000. *Int. J. Cancer* **94**, 153–156 (2001).
8. Feng, Y. *et al.* Breast cancer development and progression: Risk factors, cancer stem cells, signaling pathways, genomics, and molecular pathogenesis. *Genes Dis.* **5**, 77–106 (2018).
9. Mahoney, M. C., Bevers, T., Linos, E. & Willett, W. C. Opportunities and strategies for breast cancer prevention through risk reduction. *CA. Cancer J. Clin.* **58**, 347–371 (2008).
10. McTiernan, A., Porter, P. & Potter, J. D. Breast cancer prevention in countries with diverse resources. *Cancer* **113**, 2325–2330 (2008).
11. Mohanty, G. & Ghosh, S. N. Risk factors for cancer of cervix, status of screening and methods for its detection. *Arch. Gynecol. Obstet.* **291**, 247–249 (2015).
12. Hariri, S. *et al.* Reduction in HPV 16/18-associated high grade cervical lesions following HPV vaccine introduction in the United States – 2008–2012. *Vaccine* **33**, 1608–1613 (2015).
13. Wang, R. *et al.* Human papillomavirus vaccine against cervical cancer: Opportunity and challenge. *Cancer Lett.* **471**, 88–102 (2020).
14. de Oliveira, C. M., Fregnani, J. H. T. G. & Villa, L. L. HPV vaccine: updates and highlights. *Acta Cytol.* **63**, 159–168 (2019).
15. Chrysostomou, A., Stylianou, D., Constantinidou, A. & Kostrikis, L. Cervical cancer screening programs in Europe: the transition towards HPV vaccination and population-based HPV testing. *Viruses* **10**, 729 (2018).
16. Gallagher, K. E., LaMontagne, D. S. & Watson-Jones, D. Status of HPV vaccine introduction and barriers to country uptake. *Vaccine* **36**, 4761–4767 (2018).
17. Canfell, K. Towards the global elimination of cervical cancer. *Papillomavirus Res.* **8**, 100170 (2019).
18. Massat, N. J. *et al.* Impact of screening on breast cancer mortality: the UK program 20 years on. *Cancer Epidemiol. Biomarkers Prev.* **25**, 455–462 (2016).
19. Hu, Z. & Ma, D. The precision prevention and therapy of HPV-related cervical cancer: new concepts and clinical implications. *Cancer Med.* **7**, 5217–5236 (2018).

20. Haque, Md. M. & Desai, K. V. Pathways to endocrine therapy resistance in breast cancer. *Front. Endocrinol.* **10**, 573 (2019).
21. Rugo, H. S., Vidula, N. & Ma, C. Improving response to hormone therapy in breast cancer: new targets, new therapeutic options. *Am. Soc. Clin. Oncol. Educ. Book* **36**, e40–e54 (2016).
22. Zhu, X. *et al.* Molecular mechanisms of cisplatin resistance in cervical cancer. *Drug Des. Devel. Ther.* 1885 (2016) doi:10.2147/DDDT.S106412.
23. Yeagle, P. L. Modulation of membrane function by cholesterol. *Biochimie* **73**, 1303–1310 (1991).
24. Arora, A., Raghuraman, H. & Chattopadhyay, A. Influence of cholesterol and ergosterol on membrane dynamics: a fluorescence approach. *Biochem. Biophys. Res. Commun.* **318**, 920–926 (2004).
25. Heretsch, P. & Giannis, A. The veratrum and solanum alkaloids. in *The Alkaloids: Chemistry and Biology* vol. 74 201–232 (Elsevier, 2015).
26. Sandjo, L. P. & Kuete, V. Triterpenes and steroids from the medicinal plants of Africa. in *Medicinal Plant Research in Africa* 135–202 (Elsevier, 2013). doi:10.1016/B978-0-12-405927-6.00004-7.
27. Grattan, B. Plant sterols as anticancer nutrients: evidence for their role in breast cancer. *Nutrients* **5**, 359–387 (2013).
28. Díaz, K. *et al.* Biological activities and molecular docking of brassinosteroids 24-norcholane type analogs. *Int. J. Mol. Sci.* **21**, 1832 (2020).
29. Russo, S. *et al.* Synthesis and structure-activity relationships of amino acid conjugates of cholanic acid as antagonists of the EphA2 receptor. *Molecules* **18**, 13043–13060 (2013).
30. dos Santos, R. L., da Silva, F. B., Ribeiro, R. F. & Stefanon, I. Sex hormones in the cardiovascular system. *Horm. Mol. Biol. Clin. Investig.* **18**, (2014).
31. Stumpf, W. E. Steroid hormones and the cardiovascular system: Direct actions of estradiol, progesterone, testosterone, gluco- and mineralcorticoids, and soltriol [vitamin D] on central nervous regulatory and peripheral tissues. *Experientia* **46**, 13–25 (1990).
32. Schumacher, M. *et al.* Steroid hormones and neurosteroids in normal and pathological aging of the nervous system. *Prog. Neurobiol.* **71**, 3–29 (2003).
33. Huang, W. H. & Zheng, M. H. Steroid hormones and bone. *Histol. Histopathol.* 1257–1268 (1999) doi:10.14670/HH-14.1257.
34. Deli, T., Orosz, M. & Jakab, A. Hormone replacement therapy in cancer survivors - review of the literature. *Pathol. Oncol. Res. POR* **26**, 63–78 (2020).
35. Gil, D. *et al.* Dihydrotestosterone increases the risk of bladder cancer in men. *Hum. Cell* **32**, 379–389 (2019).
36. Majumder, A., Singh, M. & Tyagi, S. C. Post-menopausal breast cancer: from estrogen to androgen receptor. *Oncotarget* **8**, (2017).
37. Snaterse, G., Visser, J. A., Arlt, W. & Hofland, J. Circulating steroid hormone variations throughout different stages of prostate cancer. *Endocr. Relat. Cancer* **24**, R403–R420 (2017).
38. Gupta, A., Sathish Kumar, B. & Negi, A. S. Current status on development of steroids as anticancer agents. *J. Steroid Biochem. Mol. Biol.* **137**, 242–270 (2013).
39. Frank, É. & Schneider, G. Synthesis of sex hormone-derived modified steroids possessing antiproliferative activity. *J. Steroid Biochem. Mol. Biol.* **137**, 301–315 (2013).
40. Gao, W., Bohl, C. E. & Dalton, J. T. Chemistry and structural biology of androgen receptor. *Chem. Rev.* **105**, 3352–3370 (2005).

41. Cepa, M. M. D. S., Tavares da Silva, E. J., Correia-da-Silva, G., Roleira, F. M. F. & Teixeira, N. A. A. Structure−activity relationships of new A,D-ring modified steroids as aromatase inhibitors: design, synthesis, and biological activity evaluation. *J. Med. Chem.* **48**, 6379–6385 (2005).
42. Fischer, D. S. *et al.* E-ring modified steroids as novel potent inhibitors of 17β-hydroxysteroid dehydrogenase type 1. *J. Med. Chem.* **48**, 5749–5770 (2005).
43. Ling, Y. *et al.* 17-imidazolyl, pyrazolyl, and isoxazolyl androstene derivatives. novel steroidal inhibitors of human cytochrome C l7,20-Lyase (P450 17α). *J. Med. Chem.* **40**, 3297–3304 (1997).
44. Girón, R. A., Montaño, L. F., Escobar, M. L. & López-Marure, R. Dehydroepiandrosterone inhibits the proliferation and induces the death of HPV-positive and HPV-negative cervical cancer cells through an androgen- and estrogen-receptor independent mechanism: DHEA and cervical cancer. *FEBS J.* **276**, 5598–5609 (2009).
45. Ortega-Calderón, Y. N. & López-Marure, R. Dehydroepiandrosterone inhibits proliferation and suppresses migration of human cervical cancer cell lines. *Anticancer Res.* **34**, 4039–4044 (2014).
46. Jakimov, D. S. *et al.* Androstane derivatives induce apoptotic death in MDA-MB-231 breast cancer cells. *Bioorg. Med. Chem.* **23**, 7189–7198 (2015).
47. Ajduković, J. J. *et al.* Synthesis, structural analysis and antitumor activity of novel 17α-picolyl and 17(E)-picolinylidene A-modified androstane derivatives. *Bioorg. Med. Chem.* **23**, 1557–1568 (2015).
48. Djurendić, E. A. *et al.* Synthesis and cytotoxic activity of some 17-picolyl and 17-picolinylidene androstane derivatives. *Eur. J. Med. Chem.* **54**, 784–792 (2012).
49. Scherbakov, A. M. *et al.* Steroidal pyrimidines and dihydrotriazines as novel classes of anticancer agents against hormone-dependent breast cancer cells. *Front. Pharmacol.* **8**, 979 (2018).
50. Michalak, K. *et al.* Synthesis and evaluation of Na+/K+-ATP-ase inhibiting and cytotoxic in vitro activities of oleandrigenin and its selected 17β-(butenolidyl)- and 17β-(3-furyl)-analogues. *Eur. J. Med. Chem.* **202**, 112520 (2020).
51. Gyovai, A. *et al.* Antiproliferative Properties of Newly Synthesized 19-Nortestosterone Analogs Without Substantial Androgenic Activity. *Front. Pharmacol.* **9**, 825 (2018).
52. Wang, H.-L. *et al.* Synthesis and antimetastatic effects of E-salignone amide derivatives. *Drug Dev. Res.* **75**, 76–87 (2014).
53. Minorics, R. *et al.* Antiproliferative effect of normal and 13-epi-d-homoestrone and their 3-methyl ethers on human reproductive cancer cell lines. *J. Steroid Biochem. Mol. Biol.* **132**, 168–175 (2012).
54. Molnár, J. *et al.* A click approach to novel D-ring-substituted 16α-triazolylestrone derivatives and characterization of their antiproliferative properties. *PLOS ONE* **10**, e0118104 (2015).
55. Kovács, D. *et al.* Synthesis of novel 17-(4′-formyl)pyrazolylandrosta-5,16-dienes and their derivatives as potent 17α-hydroxylase/C17,20-lyase inhibitors or antiproliferative agents depending on the substitution pattern of the heteroring. *Eur. J. Med. Chem.* **120**, 284–295 (2016).
56. Mosmann, T. Rapid colorimetric assay for cellular growth and survival: Application to proliferation and cytotoxicity assays. *J. Immunol. Methods* **65**, 55–63 (1983).

57. Alföldi *et al.* Single cell mass cytometry of non-small cell lung cancer cells reveals complexity of in vivo and three-dimensional models over the Petri-dish. *Cells* **8**, 1093 (2019).
58. Kopper László & Fésüs László. *Apoptózis*. (Medicina, 2002).
59. Balog, J. Á. *et al.* Single cell mass cytometry revealed the immunomodulatory effect of cisplatin via downregulation of splenic CD44+, IL-17A+ MDSCs and promotion of circulating IFN-γ+ myeloid cells in the 4T1 metastatic breast cancer model. *Int. J. Mol. Sci.* **21**, 170 (2019).
60. Schönfeld, W. *et al.* The lead structure in cardiac glycosides is 5ß,14ß-androstane-3ß,14-diol. *Naunyn. Schmiedebergs Arch. Pharmacol.* **329**, 414–426 (1985).
61. Jourdan, F. *et al.* Effects of C-17 heterocyclic substituents on the anticancer activity of 2-ethylestra-1,3,5(10)-triene-3-O-sulfamates: synthesis, in vitro evaluation and computational modelling. *Org. Biomol. Chem.* **6**, 4108 (2008).
62. Banday, A. H., Mir, B. P., Lone, I. H., Suri, K. A. & Kumar, H. M. S. Studies on novel D-ring substituted steroidal pyrazolines as potential anticancer agents. *Steroids* **75**, 805–809 (2010).
63. Ali, M. A. *et al.* Benign synthesis of thiazolo-androstenone derivatives as potent anticancer agents. *Org. Lett.* **20**, 5927–5932 (2018).
64. Ke, S. *et al.* Synthesis and bioevaluation of novel steroidal isatin conjugates derived from epiandrosterone/androsterone. *J. Enzyme Inhib. Med. Chem.* **34**, 1607–1614 (2019).
65. Kovács, D. *et al.* An efficient approach to novel 17-5′-(1′,2′,4′)-oxadiazolyl androstenes via the cyclodehydration of cytotoxic O-steroidacylamidoximes, and an evaluation of their inhibitory action on 17α-hydroxylase/C17,20-lyase. *Eur. J. Med. Chem.* **70**, 649–660 (2013).
66. Mótyán, G. *et al.* Microwave-assisted synthesis of biologically relevant steroidal 17-exo -pyrazol-5'-ones from a norpregnene precursor by a side-chain elongation/heterocyclization sequence. *Beilstein J. Org. Chem.* **14**, 2589–2596 (2018).
67. Kovács, D. *et al.* Efficient access to novel androsteno-17-(1′,3′,4′)-oxadiazoles and 17β-(1′,3′,4′)-thiadiazoles via N-substituted hydrazone and N,N′-disubstituted hydrazine intermediates, and their pharmacological evaluation in vitro. *Eur. J. Med. Chem.* **98**, 13–29 (2015).
68. Romero-Hernández, L. L. *et al.* Synthesis of unprecedented steroidal spiro heterocycles as potential antiproliferative drugs. *Eur. J. Med. Chem.* **143**, 21–32 (2018).
69. Escriva, H., Delaunay, F. & Laudet, V. Ligand binding and nuclear receptor evolution. *BioEssays News Rev. Mol. Cell. Dev. Biol.* **22**, 717–727 (2000).
70. Dillekås, H., Rogers, M. S. & Straume, O. Are 90% of deaths from cancer caused by metastases? *Cancer Med.* **8**, 5574–5576 (2019).
71. Alizadeh, A. M., Shiri, S. & Farsinejad, S. Metastasis review: from bench to bedside. *Tumor Biol.* **35**, 8483–8523 (2014).
72. Lichterman, J. N. *et al.* A novel role for 17-B estradiol and testosterone in osteosarcoma tumorigenesis and metastasis. *J. Clin. Oncol.* **35**, e23012–e23012 (2017).
73. Boni, C. *et al.* Therapeutic activity of testosterone in metastatic breast cancer. *Anticancer Res.* **34**, 1287–1290 (2014).
74. Chiang, S. P. H., Cabrera, R. M. & Segall, J. E. Tumor cell intravasation. *Am. J. Physiol.-Cell Physiol.* **311**, C1–C14 (2016).

75. Nguyen, C. H. *et al.* 12(S)-HETE increases intracellular Ca2+ in lymph-endothelial cells disrupting their barrier function in vitro; stabilization by clinical drugs impairing calcium supply. *Cancer Lett.* **380**, 174–183 (2016).
76. Corkery, B., Crown, J., Clynes, M. & O'Donovan, N. Epidermal growth factor receptor as a potential therapeutic target in triple-negative breast cancer. *Ann. Oncol.* **20**, 862–867 (2009).
77. Zhang, P. *et al.* Upregulation of programmed cell death ligand 1 promotes resistance response in non-small-cell lung cancer patients treated with neo-adjuvant chemotherapy. *Cancer Sci.* **107**, 1563–1571 (2016).
78. Ni, J. *et al.* Epithelial cell adhesion molecule (EpCAM) is involved in prostate cancer chemotherapy/radiotherapy response in vivo. *BMC Cancer* **18**, 1092 (2018).
79. Kim, J., Kim, J. & Bae, J.-S. ROS homeostasis and metabolism: a critical liaison for cancer therapy. *Exp. Mol. Med.* **48**, e269–e269 (2016).
80. Whitaker-Menezes, D. *et al.* Evidence for a stromal-epithelial "lactate shuttle" in human tumors: MCT4 is a marker of oxidative stress in cancer-associated fibroblasts. *Cell Cycle* **10**, 1772–1783 (2011).
81. Martinez-Outschoorn, U. E. *et al.* BRCA1 mutations drive oxidative stress and glycolysis in the tumor microenvironment: Implications for breast cancer prevention with antioxidant therapies. *Cell Cycle* **11**, 4402–4413 (2012).
82. Baenke, F. *et al.* Functional screening identifies MCT4 as a key regulator of breast cancer cell metabolism and survival: MCT4 supports breast cancer cell survival. *J. Pathol.* **237**, 152–165 (2015).
83. Oh, S., Kim, H., Nam, K. & Shin, I. Silencing of Glut1 induces chemoresistance via modulation of Akt/GSK-3β/β-catenin/survivin signaling pathway in breast cancer cells. *Arch. Biochem. Biophys.* **636**, 110–122 (2017).
84. Cao, L., Chang, H., Shi, X., Peng, C. & He, Y. Keratin mediates the recognition of apoptotic and necrotic cells through dendritic cell receptor DEC205/CD205. *Proc. Natl. Acad. Sci.* **113**, 13438–13443 (2016).
85. Pulaski, B. A. & Ostrand-Rosenberg, S. Mouse 4T1 breast tumor model. *Curr. Protoc. Immunol.* **39**, (2000).
86. Schrörs, B. *et al.* Multi-omics characterization of the 4T1 murine mammary gland tumor model. *Front. Oncol.* **10**, 1195 (2020).

9 ACKNOWLEGMENTS

I would like to express my sincerest gratitudes to my supervisor, István Zupkó PhD DSc, the Dean of the Faculty of Pharmacy, University of Szeged and Head of the Department of Pharmacodynamics and Biopharmacy, for his guidance and support on this exciting but sometimes difficult path.

I am particularly thankful to Gábor Szebeni PhD whose guidance, encouragement, suggestions and very constructive criticism have contributed immensely to the evolution of my ideas on this project.

I am grateful to among others László Puskás PhD DSc from Avidin Ltd. for the help in annexin V-PI, JC-1 staining, and *in vivo* mouse model experiments.

I express my gratitude for our collaborating partners. First of all, for Éva Frank PhD and her colleagues in the Department of Organic Chemistry, University of Szeged and Suzana Jovanović-Šanta PhD and her colleagues from Department of Chemistry, Biochemistry and Environmental Protection, University of Novi Sad for the design and synthesis of the tested compounds.

I am thankful to András Szekeres PhD, from Department of Microbiology, University of Szeged, for his help in performing the YAS assay.

I express my gratitude for Georg Kruptza PhD and Kerstin Kirisits, who made it possible to learn and perform the CCIDs method and who allowed me to spend 4 months at the Department of Pathology, Medical University of Vienna.

The completion of this project could not have been possible without the participation and assistance of my colleagues and friends at the Department of Pharmacodynamics and Biopharmacy. Their contributions are sincerely appreciated and greatfully acknowledged.

Last but not the least, I would like to thank my family for their constant source of inspiration, support and their endless patience.